

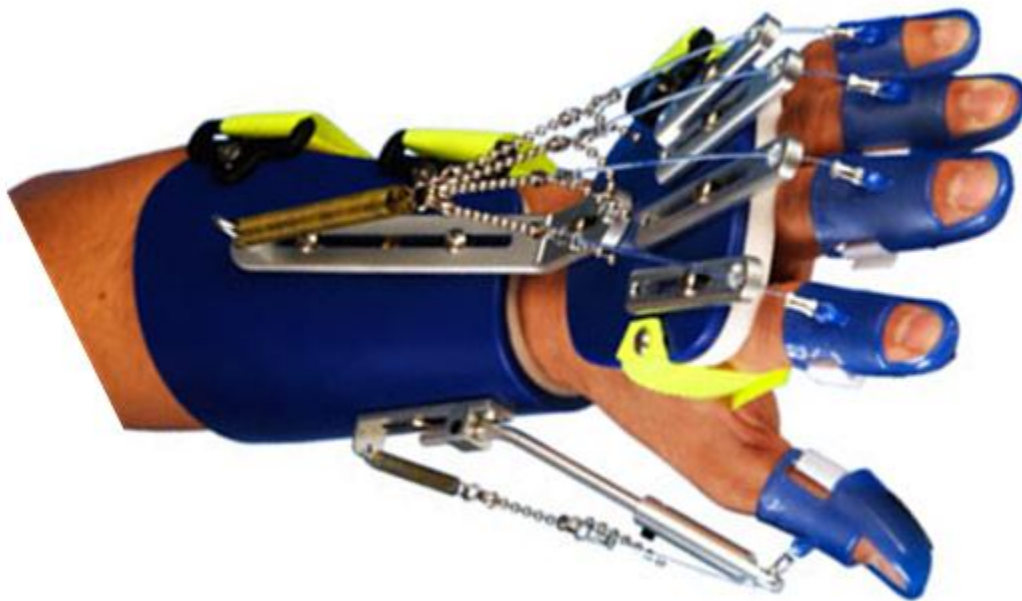
# Mirror system for hand orthoses

Internship Rik Fierkens at Hankamp Rehab Enschede

Februari 2014 – May 2014

Rik Fierkens s1004956

University of Twente



*Is it possible to create an automatic process which makes a complete 3D scan of the hand, using mirrors to obtain two simultaneous scans and a mathematical software package to combine these individual scans, to gain a custom fitted hand orthosis which can be printed by a 3D printer?*

## Titlepage

This report is meant for Hankamp Rehab and the University of Twente.

UT/WB-10.1412-17-6-10

University of Twente, MasterTrack BioMechanical Engineering,  
Postbus 217, 7500 AE Enschede, Telephone: (053)4 89 91 11

This report is written concerning STAGE of the department of BioMechanical Engineering

**Tutor:** Ir. A. Stienen

**Coordinator:** D. van de Belt

**Mentor:** F. Tönis and W. de Vries

**Date of publication:** 01-07-2014

**Publications:** 3

**Number of pages:** 66

R.I.K. Fierkens, 1004956

## Summary / Abstract

An orthosis is an externally worn mechanism for correcting misalignments or abnormal movements of the human body. It supports the human body and/or helps to reduce the rehabilitation time of a patient. Nowadays, the demand for perfect custom fitted orthoses increases thanks to the maturing technology, the need of more effective rehabilitation and the demand for more comfort for the patient. A custom fitted orthosis is a highly specialized device that is manufactured for a specific patient to meet the specific needs of the individual, so it is not suitable for another person. Because Hankamp Rehab produces several products concerning hand orthoses, the company is interested whether these products can be transformed into custom fitted orthoses to be more compliant to the customer needs. For such a transformation the geometry of the patient's hand is needed.

Previously, the traditional way of the manufacturing process of a custom fitted orthosis required a lot of time, with the involvement of several clinicians and specialists. Therefore, it is desirable to master the techniques required to make custom fitted orthoses indoors. This can be achieved by using a combination of a 3D scanner, a 3D printer and associated software. The 3D scan of the hand enables to obtain required information of the geometry of the limb and with the use of the software it is possible to print the custom fitted orthoses with the 3D printer. In order to acquire a complete scan of a limb, scans from different sides of the limb are needed. This is achieved by applying mirrors in such a way that it results in a perfect representation of the scanned surface of the human hand. The configuration and the feasibility of this solution are investigated in this report.

Firstly it was necessary to make a mathematical model of the scanning system in order to understand the scanning system better and to enable the definition of the requirements and characteristics of the different parts of this optical system. With the help of this model the assignment was further elaborated. Next the properties and the influence of the usage of mirrors were investigated; this resulted in a selection of a suitable system. Subsequently, the properties of this chosen setup were investigated and a choice was made for a total system, as robust as possible, to ensure the highest level of detail. Thereafter a prototype was built based on the principles of the theoretic system and test scans were performed with it. Besides that a combining algorithm was created to merge the scans of the different sides of the hand. Finally, a manual was made which enables Hankamp Rehab to work with this prototype and to enable further development of the system.

The goal of this report was to provide an answer to the next research question:

*“Is it possible to create an automatic process which makes a complete 3D scan of the hand, using mirrors to obtain two simultaneous scans and a mathematical software package to combine these individual scans, to gain a custom fitted hand orthosis which can be printed by a 3D printer?”*

The answer to this question is yes, it is possible, but only if many requirements are met. However, the created prototype is too primitive to perform the entire procedure in a satisfying way. Therefore it is recommended to further improve the prototype.

## Preface

This report is the written elaboration of my internship assignment at Hankamp Rehab. This internship is a compulsory part of the master's programme in Mechanical Engineering at the University of Twente. During such an internship the student can obtain practical experience within the company which he can combine with the knowledge already obtained at the University. In mutual agreement we have spread the internship over a longer period so that I was able to work too as math teacher.

This report is to demonstrate Hankamp Rehab and interested people that it is possible to obtain a full image of the human hand by means of mirrors. This report provides a good explanation of the working principles of such an optical system and gives a convincing proof of the feasibility. Furthermore, it gives a description such that Hankamp Rehab is able to work with the optical system and to enable the further development of the total system.

I would like to thank H.A. Stienen for introducing me at Hankamp Rehab and for his guidance. Also I want to thank F. Tönis for the internship opportunity and for his flexibility to let me combine this internship with my part-time work. Further I want to thank Koen Heuver for accompanying me during the project, during which he gave me a lot of valuable help with his practical insight. Furthermore, I want to express my gratitude to Marcel Heinrich for his manual in his Bachelor-Thesis and his personal support in using properly the 3D scanner, printer and the associated software. At last I wish to thank all others at Hankamp Gears and Hankamp Rehab which were involved in this assignment.

---

## Table of contents

Titlepage.....	2
Summary / Abstract.....	3
Preface .....	4
Table of contents .....	5
1 Description of the assignment.....	8
1.1 Company.....	8
1.2 Problem definition and background.....	8
1.2.1 Review of the five options.....	8
1.2.2 Discussion.....	9
1.2.3 Assignment.....	9
2 Basics of the scanning system.....	10
2.1 Working principle .....	10
2.2 Scanning in more detail .....	10
2.3 Background theory for the application of mirrors .....	11
3 Requirements and characteristics.....	12
4 Mathematical model.....	13
4.1 Model description .....	13
4.2 Determination of the lens diameters .....	14
4.3 Determination of the angles .....	15
4.4 Determination of the vertical positions of the point sources.....	15
4.5 Determination of the horizontal distance between projector and camera .....	15
4.6 Summary of the obtained mathematical model .....	16
5 Elaboration of the requirements .....	17
5.1 Distance between human hand and scanning system .....	17
5.2 Number of mirrors needed for an equal angle of incidence.....	18
5.3 Number of reflections with two mirrors.....	19
5.4 Position of the reflection on the two mirrors and the surface .....	20
5.5 Coordinate systems of the projector and the camera.....	21
6 First test design.....	22
6.1 The design .....	22
6.2 Tests.....	22
6.2.1 Variation of the scanning distance and the focus .....	22

6.2.2	Variation of the difference between camera and projector .....	23
6.3	Preliminary conclusion.....	24
7	Extended model.....	25
7.1	Added mirror system .....	25
7.2	Position of the imaginary point sources .....	25
7.2.1	Introduction.....	26
7.2.2	Determination of the coordinates for a given setup .....	26
7.2.3	Coupling between the top and the bottom mirror system.....	27
7.3	Tests with the adapted model .....	27
7.3.1	Characteristics of the bottom mirror system .....	28
7.3.2	Characteristics of the top mirror system .....	29
7.3.3	Combining the two mirror systems .....	30
7.3.4	Conforming the correctness of the total system.....	31
7.4	Discussion .....	32
8	Combining algorithm.....	33
8.1	Characteristics of the coordinate system of DAVID .....	33
8.2	Working with the OBJ file format.....	34
8.3	Simulating the manipulation of the points .....	35
8.4	Application on the scanning system.....	36
8.5	Discussion .....	37
9	Elaboration of the theoretical model.....	38
9.1	Realizing the coupling.....	38
9.2	Determination of the mirror sizes.....	39
9.3	Design of the prototype.....	40
9.3.1	The scanning system .....	40
9.3.2	The two mirrors at mirror position 1 .....	41
9.3.3	Mirror at mirror position 2.....	41
9.3.4	Mirrors at mirror position 3 and 4.....	42
9.3.5	Overview of the complete prototype .....	42
9.4	Results of the prototype .....	43
9.5	Discussion .....	44
9.6	Conclusions .....	44
10	Manual for using the total system .....	45
10.1	Preparation .....	45

---

10.2	Installation of the components in the setup.....	45
10.2.1	Top mirrors and scanning system .....	45
10.2.2	Bottom mirrors .....	47
10.2.3	Placement of the desired scan object.....	47
10.3	Control and performance of the scan.....	48
11	Conclusion and recommendations.....	49
12	References .....	50
13	Generated software .....	51
A.	Appendices .....	52
I.	Appendix A1 Relationships of the mirrors.....	53
II.	Appendix A2 Position of the imaginary point sources .....	54
III.	Appendix A3 Independency of the top mirror parameter .....	59
IV.	Appendix A4 Reducing the equations for the imaginary points sources.....	61
V.	Appendix A5 Calculation of the minimum and maximum first mirror distance .....	63
VI.	Appendix A6 Calculation of the minimum vertical tilt angle .....	65

## 1 Description of the assignment

In this section the company and the assignment will be discussed.

### 1.1 Company

Hankamp Rehab is a company which emanated from Hankamp Gears. Hankamp Gears is a producer of high quality gears for different industries for over more than 100 years. The subsidiary company, Hankamp Rehab, is specialized in rehabilitation technology. The reasons for forming this company in 2009 were the contacts with the University of Twente and a trade mission by the United States. It turned out that there was (and still is) a need for a market participant for innovative rehabilitation products, not only within the Benelux region but worldwide. Therefore they have become not only the official distributor of Saebo products in the Netherlands and Belgium, but they also produce and export Saebo products worldwide. For Saebo they also organize training sessions for rehabilitation physicians to work with the Saebo products. Examples of Saebo products are the SaeboSTRETCH, the SaeboFLEX, the SaeboREACH and the SaeboMASS [1].

Besides distributing Saebo products and services all over the world, they also have an engineering department where the different Saebo products are innovated and tested. Furthermore they can make use of the neighboring factory and the network of suppliers of Hankamp Gears. Hence, next to distributing rehabilitation products, their other vision is to develop and design, produce and launch rehabilitation products on the worldwide market. An example of this is the SaeboMASS which was developed here in 2011 and nowadays has a more compact version. Moreover they have an ambition to grow in size and move into the nearby building with empty offices.

### 1.2 Problem definition and background

A large share of the products at Hankamp Rehab are orthoses. Because these products have to work well on all patients, there is need for custom fitted components. Previously, in the traditional way this procedure took a lot of time with the involvement of several clinicians and specialists. Therefore it is desirable to master the techniques required to make custom fitted orthoses indoors. This can be achieved by using a combination of a 3D scanner, a 3D printer and associated software. The working principle and proof of this method are described in reports of previous interns Marcel Heinrich and Johannes van Wijngaarden [2,3].

The 3D scan of a limb makes it possible to get the needed information of the geometry of the limb and with the use of the software it is possible to print the custom fitted orthoses with the 3D printer. But in order to obtain a complete scan of a limb, scans from different sides of the limb are needed. Besides, every scan has to be made in the exact same configuration every time, otherwise it will not be possible to fuse the scans together. Therefore it is almost necessary to make sure the object you are scanning is fixated. If you want to get a complete scan of a limb there are several possibilities [3]:

1. Fixate the limb and take several scans at different angles
2. Make several scans really fast after each other
3. Make a mold of the limb and scan the mold
4. Scan from different angles at the same time
5. Other solutions where multiple scanner systems are involved

#### 1.2.1 Review of the five options

The first option is the most primitive option and is possible, but the fact that there have to be taken multiple scans at different angles is time-consuming. Moreover, this entails a complex condition with it. The setup for the different scans has to be comparable with each other otherwise the results are not reliable. Also the comfort of the patient and the influence of the fixating parts in the scan should be taken into consideration. This all makes the first option unfeasible.

The second possibility is investigated by a previous intern, by applying an advanced camera system which rotated around the limb as fast as possible while taking several scans. By using this possibility the problem of comparable scans, which was a complex condition at the first possibility, is tackled because the scans are all taken at the same radius. Unfortunately, the conclusion of this research was that this is not a feasible solution and the results are not as good as desired [3].

Regarding the third option, making a gypsum mold is a difficult and a time-consuming task. Therefore previous interns used a clay like material which is also a children's toy, Bouncing Putty. It is a very malleable material which holds its shape after being formed. Furthermore it is able to make an imprint even of fingerprints so the amount of detail which the mold can retain is sufficient for making well fitting orthoses. Although it is possible to make a double sided mold which completely encloses a limb, it proved extremely difficult to make a complete 3D image of the molds. So it is preferable to look at other solutions [3].

For the fourth possibility where simultaneously scans are made at different angles, there will be made use of mirrors. When splitting the scan beam in different parts and guide these separate beams with the use of mirrors on different spots of the limb, it is theoretically possible to get a complete scan of the limb. When it is known how the images of these different (part)scans are created it is possible to fuse these different images into a full 3D image of the limb. This interesting possibility has not been investigated yet.

The last option requires multiple scan systems, but Hankamp Rehab has only one scan system in possession. A new system costs around 2000 euro's and therefore this solution is not tested during my internship [4].

### 1.2.2 Discussion

A significant problem all previous interns encountered was the joining of the different scans by the supplied software. The software looks at two scans and tries to find the largest area they have in common and places them on each other. With irregular shaped objects this works very well. However when having a regular shaped object as scan, the software joins them in a way which is mathematically correct, but doesn't match reality. Besides that, enough overlap is needed between these scans so that the different scans can be joined together easily with the supplied software, preferably six scans [3]. To avoid these problems and to be able to gain a complete 3D scan of a limb with less different scans, a new piece of software has to be written which combines scans on a basis of orientation of the points in space instead of geometry similarity.

For the Saebostretch and Saeboflex it is useful to gain 3D images of a patient's hand to be able to create custom fitted components for these products. When this can be achieved by using a method where scans from different angles at the same time are combined and processed with a software package, this will result in an efficient and time-saving way of hand orthoses making.

### 1.2.3 Assignment

When combining the knowledge and perspective mentioned above one arrives to the following question: Is it possible to create an automatic process which makes a complete 3D scan of the hand, using mirrors to obtain two simultaneous scans and a mathematical software package to combine these individual scans, to gain a custom fitted hand orthosis which can be printed by a 3D printer?

The assignment of my internship is to answer this research question. The interesting idea is that if the working principle of this method can be proven with two simultaneous images created by mirrors, then a more advanced setup with more mirrors and images is also possible. The ideal future situation is a product where a patient puts his hand in shortly, during which a complete hand scan is made and just several hours later a custom fitted hand orthosis is ready for use on the patient.

## 2 Basics of the scanning system

Before one is able to investigate the 3D-scanning in combination with mirrors, firstly there must be looked closer to the details of the assignment.

### 2.1 Working principle

The procedure of 3D scanning and printing consists of three main steps:

- The first step is to create a scan of the patient's hand which is detailed enough to enable the creation of a perfect fitted orthosis for the specific patient. This is established with the scanning setup of DAVID [4,5]. The hardware consists of a mounting rack on a tripod on which a high resolution projector and camera are mounted. The enclosed software enables to make scans. The working principle will be discussed in the next section.
- The second step is to edit and adjust the obtained scan or scans. This can be carried out with the provided software, but also with other programs like Blender, Meshlab and Matlab. This further processing is desired to delete unwanted noise or parts of the scan and to fuse multiple parts of a scan (or multiple scans). The step ends with a file which can be sent to the 3D printer.
- The last step is to print the processed 3D image with the 3D printer. This will be done by the Ultimaker and the associated software Cura (a 3D printer and associated software) [6]. This is a simple execution which only has to be initiated and once started does not need to be looked after. The time of this operation depends heavily on the size of the orthosis.

In the assignment I looked intensively to the first two described steps and did not pay attention to the last step because this is not influenced by the presence of mirrors in the system. In this report I will describe how these first two steps are influenced by the presence of mirrors and in what way these steps have to be adapted to achieve that the whole procedure is operating correctly.

### 2.2 Scanning in more detail

In Figure 2.1 on the right a detailed view of the different components of DAVID's scanning system is shown. In the figure the mounting rack is shown with the camera and the projector mounted on it. These components must be connected to a computer and the projector also to a power supply. With the use of the software located on an usb-drive it is possible to make scans. The distance between these two components and the orientation of it depends both on the total size of and the distance to the scanned object. That is the reason why the system is a modular setup and its configuration can be adjusted.

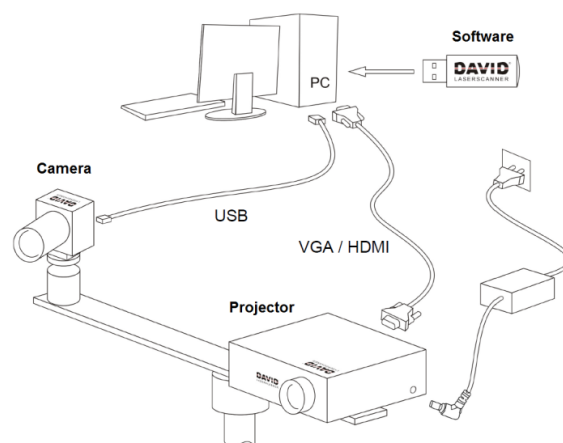


**Figure 2.1** Overview of the DAVID scanning system

The software needs to be fed with the location and the orientation of these two components in order to be able to perform scans. As a consequence, the system must be calibrated [5]. This part is done with the use of a calibration corner as reference, whose characteristics are known precisely. The mounting rack must be placed in front of the scanned object and the position and the direction of the projector have to be adjusted such that its projection illuminates the surface to be scanned. After this the mounting rack can move and rotate, while the camera and projector stay fixed. In this way the system is fully calibrated now.

The working principle of the system is as follows: The projector projects different patterns on the scanned object in such a way that the camera can monitor the deformations of these patterns,

caused by the relief of the object, so that a 3D surface becomes created. This surface can be adjusted and edited by software programs to establish a full 3D image which can be printed by the 3D printer. During the combination of multiple scans it is essential that the scans are obtained from the same calibration setup and from a comparable scan setup [3].

For further information and a more extensive description reference is made to the Bachelor-Thesis of Marcel Heinric [2]. This report contains a clear step-by-step-guide to allow people, which do not have any experience in the field of 3D scanning and 3D printing, to successfully use these techniques to create custom fitted components for orthoses with the use of the discussed software and hardware.

### **2.3 Background theory for the application of mirrors**

If the reflecting surface is very smooth, like in the case of mirrors, the reflection of light that occurs is called specular or regular reflection. The laws of reflection are then as follows:

- The incident ray, the reflected ray and the normal of the reflection surface at the point of incidence all lie in the same plane.
- The angle that the incident ray makes with the normal is equal to the angle that the reflected ray makes with the same normal.
- The reflected ray and the incident ray are on the opposite sides of the normal.

In addition, refraction of light will occur because the mirrors aren't infinitely thin, but are covered with glass which has a certain thickness. During the transition of a beam of light from one to the other transparent medium refraction of light takes place. The refraction angle does have a different value than the incident angle. There is a constant goniometric ratio between these two angles, named the refraction index. This is stated in the law of Snellius [7].

These laws of reflections and refraction will be applied during the design and the placement and orientation of the mirrors. These principles enable the definition of point sources, with which it becomes able to understand the working principles and applied adaptations of the scanning system.

### 3 Requirements and characteristics

This chapter offers a list of the requirements and characteristics that will serve as guidelines for the creation of a scanning system that is able to make a full 3D image of the human hand.

- It must be a time-saving process:  
The process must be efficient and smoothly in order that custom fitted parts of the orthoses can be created as less time-consuming as possible. This also means that the total system should be designed as simple as possible.
- The system must be able to scan a whole hand of different patients:  
As a first consequence the range of the camera and the projector must be set properly. This condition determines to a large extent the size of the entire system. Secondly, the system must be automatically adjustable so it is able to scan different human hands.
- The hand must be static:  
In this way a situation will be achieved that makes it possible to combine the scans in a later stage. This means that the hand of the patient has to be supported without disrupting the process.
- Usage of mirrors to obtain two sides of the human hand:  
Mirrors will be used to enable the system to make two scans simultaneously. In this way the system can combine these scans in a later stage to establish a complete 3D image of the hand. The laws of reflections will be used to design the system.
- Controlled reflections:  
Because almost everything around us reflects light, special attention must be paid to the objects present in the system. The only objects that may reflect are the mirrors, so that in this way no unwanted reflections can occur.
- The calibration process must stay executable:  
The system will be extended with mirrors and supporting constructions; these objects may not interrupt the calibration process.
- Good quality of the scans:  
The influence of natural light (sunlight) and other ambient (artificial) light is very noticeable. If they change, then the measurements become unusable. As a result, it is desirable to control the degree of ambient light in the system. Furthermore, the projector and the camera must be well focused. In this way a situation is achieved where these two components operate with optimal settings.
- The scanning procedure should be repeatable:  
This means that the setup must be designed durable and the setup has to be protected against dust and other things and situations that can disrupt or influence the process in a negative way.
- The scans obtained by the measurements must be combinable:  
A situation must be created where the software knows where the two scans are located relative to each other in space, so that an algorithm can combine these scans in a proper way.

### 4 Mathematical model

In order to understand the scanning system better and to be able to qualify the requirements and characteristics of the different parts of this system, a sound mathematical model of the system is needed. Such a model becomes possible by making some assumptions. With the help of this obtained model the assignment can be further elaborated.

#### 4.1 Model description

The most important assumption is that both the projector and the camera are point sources located behind their lenses in the same orientation plane. The 2D mathematical model of these two hardware components is shown in Figure 4.1. With this assumption the behavior of the light beams of both the projector and the camera can be modeled and predicted. To fully define an appropriate mathematical model all the characteristics of these components have to be determined, as shown in Figure 4.1 on the right.

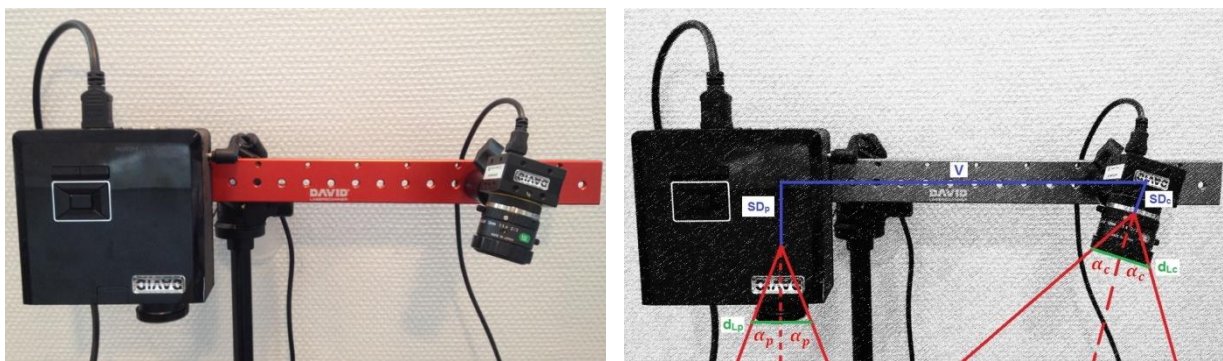


**Figure 4.1** On the left a front view of the setup with the mounting rack in a vertical position; on the right the mathematical model for the same setup with the assumption that there are two imaginary point sources

To define the projection angle  $\alpha_p$ , camera angle  $\alpha_c$ , the virtual lens diameters ( $d_{Lp}, d_{Lc}$ ), the heights relative to the red mounting rack (defined as  $SD_p$  and  $SD_c$ , respectively) of these two point sources and the horizontal distance  $V$  between these points, several measurements are done by varying the height between the red mounting rack and the projection surface. For these measurements the basic setup is identical to the one presented in Figure 4.1.

By varying the height the size of the projection area and the camera view range are manipulated. During each scanning action the projection patterns are as illustrated in Figure 4.2 and 4.3. The projector always projects a rectangular image which is tilted in one direction, as shown in Figure 4.3.

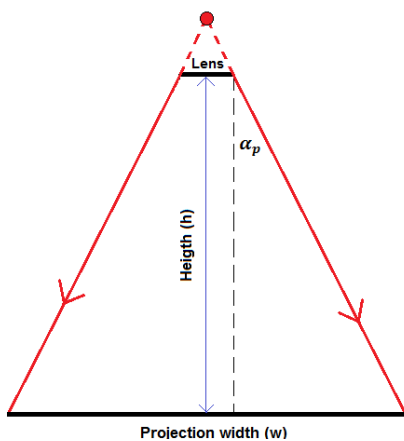


**Figure 4.2** Front view of the projection pattern

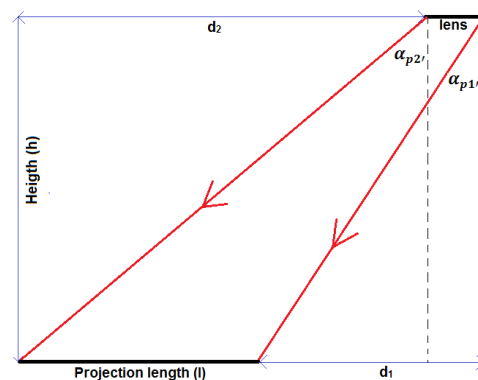


**Figure 4.3** Side view of the projection pattern

The camera captures an image for which the centre is directly below the centre of the lens. This ensures that not only the front view of the camera is as depicted in Figure 4.2, but also the side view. It should be noted that the camera angle of the front view ( $\alpha_c$ ) is different from the one of the side view ( $\alpha_{c'}$ ), because the captured image is by definition rectangular. The consequences of these properties are illustrated in Figure 4.4 and 4.5

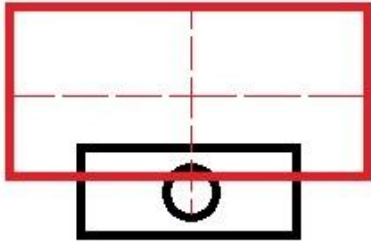


Figure 4.4 Front view of the projector

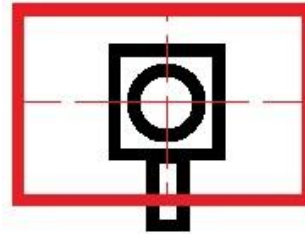


Figure 4.5 Front view of the camera

In Figure 4.4 the projection of the projector is shown in red and in Figure 4.5 the captured image of the camera is shown in red. Both ranges are rectangular, but the big difference is that the centre of the projection does not coincide with the centre of the projection lens, although this is the case for the camera. Therefore the camera situation is simpler than that of the projector.

By using the characteristics defined in Figure 4.2 and 4.3 and the diameters of the lens  $x$  ( $d_{Lx}$ ) the angles can be defined as follows (making use of trigonometry):

$$\alpha_x = \tan^{-1} \left( \frac{w - d_{Lx}}{2h} \right) \quad [\text{valid for } \alpha_p, \alpha_c \text{ and } \alpha_{c'}]$$

$$\alpha_{p1'} = \tan^{-1} \left( \frac{d_1}{h} \right)$$

$$\alpha_{p2'} = \tan^{-1} \left( \frac{d_2}{h} \right) = \tan^{-1} \left( \frac{l + d_1 - d_{Lc'}}{h} \right)$$

### 4.2 Determination of the lens diameters

The calculations and operations in the next sections of this chapter will be done in Matlab [M1,M2].

The obtained equations contain the virtual diameters of the lenses ( $d_{Lx}$ ) and therefore they are needed. These values are determined during the iterative process with the precondition that the equations are equal at the different heights. This means that the estimation error, the difference between the angles at the different heights, is minimized; this is shown in Figure 4.6 and 4.7 below.

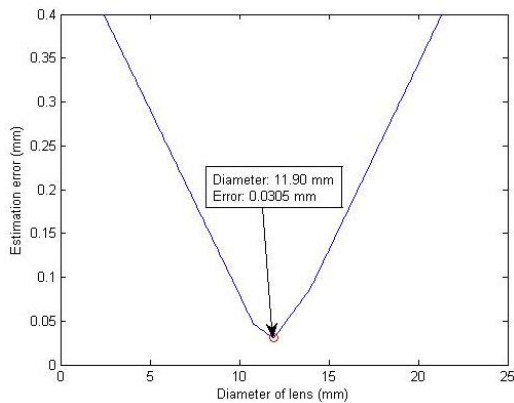


Figure 4.6 Determination of the optimal diameter of the projector lens:  $d_{Lp} = 11.90$  mm

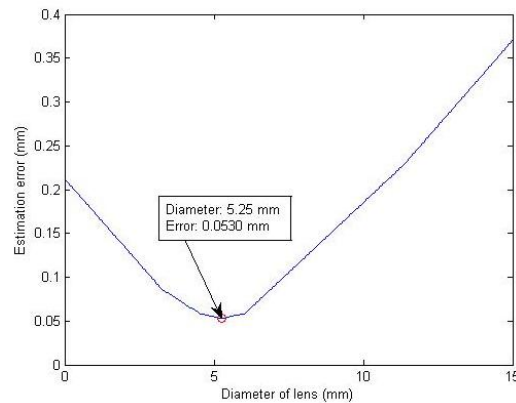


Figure 4.7 Determination of the optimal diameter of the camera lens:  $d_{Lc} = 5.25$  mm

### 4.3 Determination of the angles

Filling in these optimal diameters in the obtained equations gives values for the angles, the results are shown in Table 4.1 below.

**Table 4.1** The calculated angles of the projector and the camera (done in Matlab)

	Projector	Camera
Front view	$\alpha_p = 12.2969^\circ$	$\alpha_c = 11.2667^\circ$
Side view	$\alpha_{p1'} = 2.0796^\circ$ $\alpha_{p2'} = 19.8109^\circ$	$\alpha_{c'} = 9.5242^\circ$

### 4.4 Determination of the vertical positions of the point sources

Using the optimal lens diameters and the obtained angles makes it possible to calculate the heights relative to the red mounting rack ( $SD_p$  and  $SD_c$ ). With the knowledge that the distance between the outer edge of the projector and the centre of the mounting rack is 90 mm and that from the centre to the outer edge of the camera is 40 mm (measured values),  $SD_p$  and  $SD_c$  can be calculated.

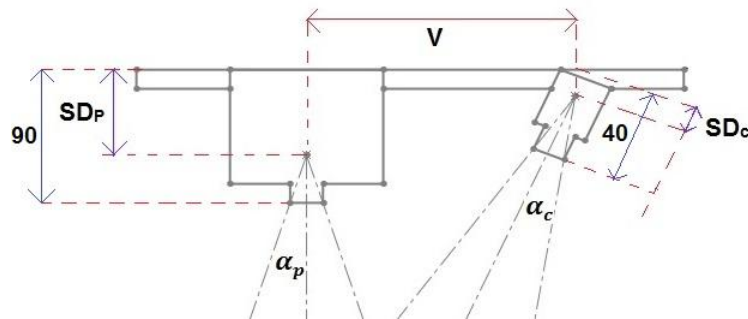


**Figure 4.8** Position of the point sources in the scanning system

Using Figure 4.8 gives:

$$SD_p = 90 - \frac{d_{Lp}}{2 \tan(\alpha_p)} = 62.7038 \text{ mm}$$

$$SD_c = 40 - \frac{d_{Lc}}{2 \tan(\alpha_c)} = 26.8233 \text{ mm}$$

### 4.5 Determination of the horizontal distance between projector and camera

In the user manual of the DAVID system a table is listed which gives indications for the distance between the camera and the projector ( $V$ ), depending on the distance between scanner and object ( $E$ ), such that this results in an optimal setup. To validate these values and to enable the processing of these optimal settings in the mathematical model, these values are plotted and then curve fitting is used to obtain an equation. This resulted in the graph which is plotted in Figure 4.9 on the right (made in Matlab [M3]).

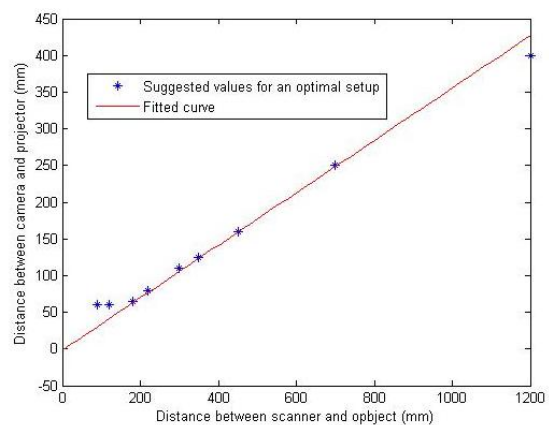


**Figure 4.9** Obtained linear relationship between the two distances ( $V$  and  $E$ ) for of an optimal setup

This results in the following linear equation:

$$V [mm] = 0.35714 \times E[mm] - 1.42857$$

#### 4.6 Summary of the obtained mathematical model

With all these obtained values the mathematical model is complete and the assignment can be elaborated. The small estimation errors are negligible and therefore this mathematical model can be considered as correct. The properties of the mathematical model are summarized in Table 4.2 below.

**Table 4.2** Summary of the obtained values for the mathematical model

Characteristic	Projector	Camera
Angle front view	$\alpha_p = 12.2969^\circ$	$\alpha_c = 11.2667^\circ$
Angle side view	$\alpha_1 = 2.0796^\circ \quad \alpha_2 = 19.8109^\circ$	$\alpha_{c'} = 9.5242^\circ$
Diameter lens	$d_{Lp} = 11.90 \text{ mm}$	$d_{Lc} = 5.25 \text{ mm}$
Height relative to mounting rack	$SD_p = 62.7038 \text{ mm}$	$SD_c = 26.8233 \text{ mm}$
Distance between projector and camera	$V = 0.35714 \times E - 1.42857$ (V and E in mm)	

## 5 Elaboration of the requirements

In this section the requirements and characteristics of the system will be further elaborated with the use of the obtained mathematical model in the previous chapter.

### 5.1 Distance between human hand and scanning system

From the demand that a whole human hand can be scanned, as described in section 3, the size of the projection area can be determined. Therefore the dimensions of human hands are required, the important dimensions of the human hand are shown in Table 5.1 below.

**Table 5.1** Important dimensions of the human hand, where the columns containing “DINED” represent the characteristic values for the Netherlands [8].

populations	DINED 2004 (20-60 years), mixed		DINED 2004 (20-60 years), male		DINED 2004 (20-60 years), female		International, mixed		International, male		International, female	
	P50	P95	P50	P95	P50	P95	P50	P95	P50	P95	P50	P95
43. hand length (mm)	187	208	196	214	178	191	170	199	185	200	155	170
47. hand breadth (with thumb) (mm)	103	118	112	120	93	103						
48. hand thickness (mm)	26	36	29	34	27	35						

As can be seen in Table 5.1, the average hand size in the Netherlands is larger than the average world value. Dutch males have the biggest hands and therefore these values will be used for the determination of the size of the projection area. Also the fact that both sides of the hand, the top and bottom side, have to be scanned influences the dimensions of the projection area. The image of the projector has to cover the scanned object, so this means the bottom and top side of the hand. Therefore it is assumed that at least the half of the projection area has to be reserved for enabling coverage of the other side of the hand. This is illustrated in Figure 5.1.

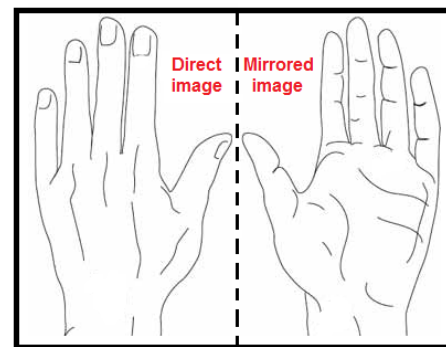


**Figure 5.1** Projection area filled with the hand as visible by the camera.

According to Table 5.1, Dutch males possess the biggest hands. Their maximum hand length is 214 mm and the hand breadth is 120 mm. The ratio between the length and the width of the projection area makes it logical to position the hand in the orientation as shown in Figure 5.1. In this way the hand length determines the dimensions of the projection area. In other words; when the hand length fits in the projection area, the hand breadth fits automatically. Therefore the length of the projection area is set at 220 mm to realize a safety margin of 6 mm.

With the use of both this value and Figure 4.3 in Chapter 4 it is possible to determine the minimum scanning distance (distance between the outer edge of the projector lens and the scanned object) :

$$E_{min} = \frac{220 - d_{lensp}}{\tan(\alpha_{p2}) - \tan(\alpha_{p1})} = 645.5171 \text{ mm}$$

With this value it becomes possible to determine the distance to the projector's point source ( $D_{min}$ ) and the length of the projection area:

$$D_{min} = E_{min} + (90 - SD_p) = 672.8133 \text{ mm}$$

$$\text{Width projection area (w)} = 2[\tan(\alpha_p) * D_{min}] = 296.0878 \text{ mm}$$

The value of the length of the projection area confirms that the hand breadth fits easily two times within the projection area. The distance between the scanning system and the scanned object is preferably as small as possible in order to have the highest resolution, but in order to obtain a simple setup and an extra safety factor the scanning distance (E) will be fixed at 650 mm.

**5.2 Number of mirrors needed for an equal angle of incidence**

*Note: During the analyses in Section 5.2 until Section 5.4 only attention is paid to the behavior of the projector. This is done because the properties of the camera are comparable, the only difference is that the camera is at a different position and has a different orientation.*

With the obtained value of the scanning distance E, calculated in section 5.1, a simplified setup arises. This setup is illustrated in Figure 5.2. In this figure the dotted blue line represents the projection surface and the red lines the projector/camera beams. The solid red lines are needed for the capturing of the top side of the human hand and the dotted red lines for the bottom side. To enable the capture of the bottom side of the human hand, mirrors are needed that reflect these dotted lines. These two images need to be combined in a later phase. In case the angles of incidence<sup>1</sup> of the bottom and top side are equal, two advantages appear; the effort of the combining process is minimized since the rotation of the two images is prescribed easily and the level of detail of the total image is optimized. Therefore a mirror setup is needed that offers this property.

To enable this desired behavior, the influences of the number of used mirrors must be investigated. For this purpose four situations will be analyzed and discussed afterwards: a mirror setup consisting of one mirror, two mirrors, three mirrors and four mirrors. To enable a comparison of these different situations parameters will be introduced, see Table 5.2 and Figure 5.3. The figure shows the four mirrors and their inclining angles for a mirror setup consisting of four mirrors, the blue line represents the projection surface again.

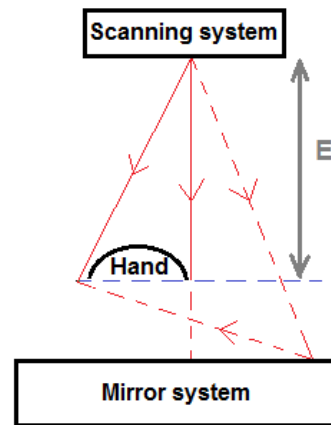


Figure 5.2 Simplified 2D setup

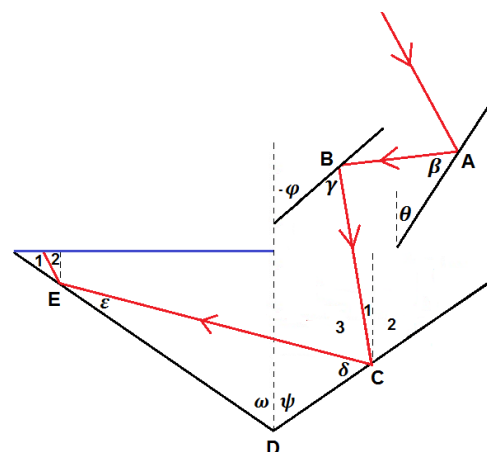


Figure 5.3 Inclining angles of the mirrors

**Table 5.2** Parameters of the different mirrors (inclining angles are the angles with the vertical)

$\alpha$ : the projection angle of the projector (angle between vertical and projection beam)	
$\beta$ : the angle of incidence on the first mirror	$\theta$ : the inclining angle of the first mirror
$\gamma$ : the angle of incidence on the second mirror	$\varphi$ : the inclining angle of the second mirror
$\delta$ : the angle of incidence on the third mirror	$\psi$ : the inclining angle of the third mirror
$\epsilon$ : the angle of incidence on the fourth mirror	$\omega$ : the inclining angle of the fourth mirror

The angles in Table 5.2 are related to each other and hence can be expressed in relationships. This property will be used in the analysis of the different situations. These analyses are done in Appendix I and result in boundary conditions which are summarized in Table 5.3 on the next page.

<sup>1</sup> angle of incidence: angle of the projector/camera beam that hits the projection surface

**Table 5.3** Boundary conditions for a same angle of incidence for the different setups

Number of mirrors used in setup	Boundary condition for same angle of incidence
One mirror	$\theta = 90^\circ - \alpha$
Two mirrors	$\varphi + \theta = 90^\circ$
Three mirrors	$\psi + \theta + \varphi = 90^\circ - \alpha$
Four mirrors	$\psi + \omega + \theta + \varphi = 90^\circ$

This table shows that the boundary conditions of situations with one or three mirrors contain the parameter  $\alpha$  and that this is not the case for situations with two or four mirrors. Also a strong resemblance exists between the boundary conditions for situations with one and three mirrors on the one hand and the situations with two and four mirrors on the other hand. Therefore it can be concluded that there is a principal difference for situations with an even and odd number of mirrors.

In case of an odd number of mirrors, the boundary equation is dependent of the projection angle  $\alpha$ ; as a consequence, each lightray requires a different specific mirror orientation and this is physically not possible in practice. Therefore such an optical setup is infeasible.

On the contrary, in case of an even number of mirrors the boundary equation is independent of the projection angle  $\alpha$ . Hence, it can be concluded that when a system is chosen with any even number of mirrors, the requirement of same angle of incidence is fulfilled. In order to reduce the complexity of the optical system and to reduce the influence of refraction by the mirrors, a mirror system with the minimum amount of two mirrors is chosen. This system will be used in the further elaboration.

**5.3 Number of reflections with two mirrors**

In the previous section a two mirror system was chosen as basis. To achieve the requirement of an equal angle of incidence, each beam must intersect these two mirrors one time. This is illustrated in Figure 5.4.

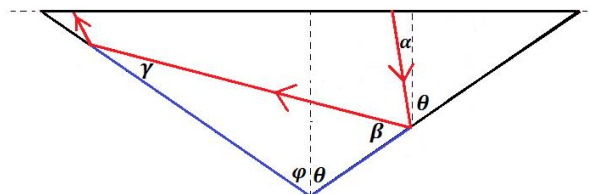


**Figure 5.4** The two mirrors below the projection surface and the impingement of a random beam

When using this requirement in combination with the parameters indicated in the figure, some boundary conditions arise for the number of reflections (assuming that the mirrors have infinite dimensions) :

Only one reflection on the mirrors (beam misses the second mirror):

$$\begin{aligned} \beta - (90^\circ - \theta) &> 90^\circ - \varphi \\ 2\theta + \alpha - 90^\circ &> 90^\circ - \varphi \\ 2\theta + \varphi &> 180^\circ - \alpha \end{aligned}$$

More than two reflections (reflected beam of the second mirror hits the first mirror again):

$$\begin{aligned} (180^\circ - \gamma) - (90^\circ - \varphi) &< (90^\circ - \theta) \\ (180^\circ - (180^\circ - 2\theta - \alpha - \varphi)) - (90^\circ - \varphi) &< (90^\circ - \theta) \\ 2\theta + \alpha + 2\varphi - 90^\circ &< 90^\circ - \theta \\ 3\theta + 2\varphi &< 180^\circ - \alpha \end{aligned}$$



### 5.5 Coordinate systems of the projector and the camera

The requirements that a least the half of the projection area has to be used for the reflection, and that the combining process of the two obtained images has to be as simple as possible, have influence on the orientation of the camera. This would entail that the coordinate system of the projector must be coincided with the coordinate system of the camera. With the use of Figure 5.6 it is then possible to define the inclining angle of the camera:

In Section 4.5 the following equation was obtained:

$$V = 0.35714E - 1.42857$$

Applying this to the figure gives for the inclining angle ( $\lambda$ ):

$$\lambda = \tan^{-1}\left(\frac{E + 90}{V}\right) = \tan^{-1}\left(\frac{E + 90}{0.35714E - 1.42857}\right)$$

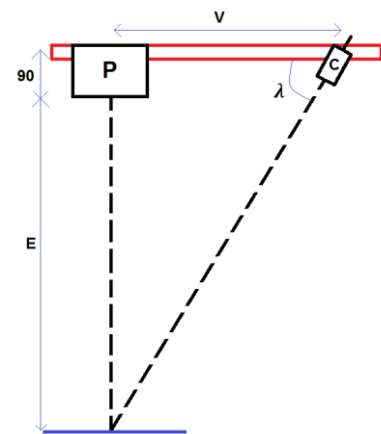


**Figure 5.6** The needed setup of the projector (P) and camera (C)

## 6 First test design

With the knowledge obtained from the elaboration of the requirements in Chapter 5 it is possible to create a primitive test design.

### 6.1 The design

In this section the design of the system and the important characteristics of the system will be presented and explained. In Figure 6.1 the 2D test design is illustrated. The figure contains parameters which can be varied and also parameters which are constants and which were determined in the previous Chapters 4 and 5.

Constant parameters:

$$SD_p = 62.7038 \text{ mm}$$

$$SD_c = 26.8233 \text{ mm}$$

$$\alpha_c = 11.2667^\circ$$

$$\alpha_p = 12.2969^\circ$$

Parameters that can be chosen:

- A and B:

The horizontal and the vertical distance between the inclining point of the mirrors and the centre of the coordinate system of the scanning system.

- $\theta$  and  $\varphi$ :

The inclining angles of the two mirrors.

- E:

The height of the lens of the projector and the projection surface (scanning distance).

Dependent parameters:

$$V = 0.35714E - 1.42857$$

$$\lambda = \tan^{-1} \left( \frac{E + 90}{0.35714E - 1.42857} \right)$$

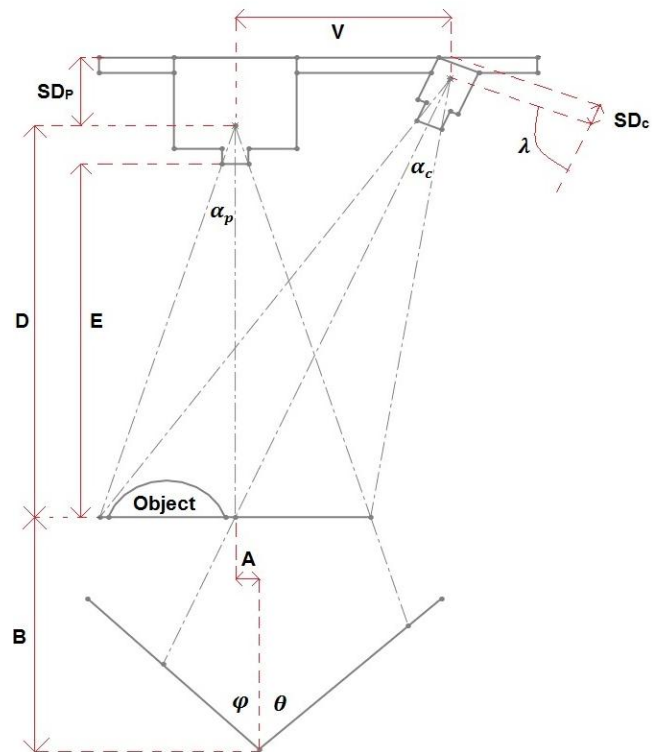


Figure 6.1 An overview of the test design

This means that if the height of the scanning system (E) and the orientation and the position of the mirrors are chosen (A, B,  $\theta$  and  $\varphi$ ), the setup is fully defined. In the following section it is investigated what the influence is of the parameters that can be chosen.

### 6.2 Tests

To investigate the influences of characteristic elements of the mirror arrangement, several tests are done. During these tests changes were applied one by one, while the rest of the arrangement remained unaffected. The execution and the results of these tests are listed in this section.

#### 6.2.1 Variation of the scanning distance and the focus

During this test use is made of a setup which is fully calibrated for a certain scanning distance (E) and for subsequently making scans at different distances (which are not equal to E). In this way the influence of a deviation in the scanning distance can be investigated. Furthermore after the making of a scan at a deviated height the focus of the scanning system is adapted to such a situation that enables to say something about the influence of focus. In this test the mirrors are not used, in order to make sure that the scan is not influenced by them. Of course this means that only a scan of the top of the hand is made.

The setup is calibrated at a scanning distance of 650 mm and afterwards the distance is varied to 660 mm and 640 mm, so an absolute deviation of 10 mm is applied. From these different scans the length of the middle finger and the total width of the middle and the ring finger are measured as characteristic lengths, to enable a comparison of the different scans. Besides that, the number of (mesh) faces that are present in the scans are used to compare the scans on detail. The results of this procedure are displayed in Table 6.1.

**Table 6.1** The results of scanning one human hand at different heights and/or different focus

Height E	Number of faces	Width of the two fingers	Length middle finger
650 mm	2085194	40,35 mm	85,25 mm
750 mm	1924655	41,25 mm	86,32 mm
750 mm refocused	1942350	39,03 mm	84,55 mm
450 mm	1601166	38,65 mm	81,32 mm
450 mm refocused	1547576	40,68 mm	86,05 mm
<b>Real dimensions of the hand</b>		approx. 40 mm	approx. 85 mm

The first things that stand out from the scans that are made at heights which are too large is that the colors become dull and gray. Looking at the measurement results in Table 6.1 it can be concluded that it is important to calibrate and scan at the same distance otherwise significant deviations will occur. Also the refocusing of the scanning system leads to problems in the scans, because the characteristic dimensions deviate a lot by doing this and therefore the scans are not reliable anymore.

### 6.2.2 Variation of the difference between camera and projector

During this test use is made of a setup which is fully calibrated for situations with a different distance between the scanner and projector (V). In this way it can be investigated if it is necessary to obey the values listed in the manual, so set the distance E according to the obtained equation for V. In the mounting rack a pattern of screw holes is present. During this test the camera is continuously attached in another hole, subsequently the system is calibrated and a scan is made. This scans are in a same way analyzed as in the previous test; the results are listed in Table 6.2 below.

**Table 6.2** The results of scanning with a different distance between projector and camera

Distance V	Number of faces	Width of the two fingers	Length middle finger
3 screw holes	1987947	40,41 mm	84,99 mm
5 screw holes	2076807	40,22 mm	84,78 mm
7 screw holes (optimal)	1972081	39,78 mm	84,42 mm
9 screw holes	1850858	40,08 mm	85,93 mm
11 screw holes	1721443	40,13 mm	85,97 mm
13 screw holes	1605804	39,81 mm	84,41 mm
15 screw holes	1505337	39,84 mm	84,67 mm

At first glance, there are no significant differences to discover between the images of the various scans. What do change are the color and the fine detail. When the distance (V) is equal to (or near) the optimal distance, according to the mentioned equation, the fine details are best observable and the colors are the most natural. Besides that, when the distance is greater than the optimal distance, the camera angle decreases and the image is captured at a larger angle. The consequence of this is that there exists more shadow in these scans.

Looking at the measurement results in Table 6.2 it can be concluded that there is no significant difference in the characteristic dimensions of the hand. But visible are the differences between the number of faces, this value decreases with increasing difference of V. This can be linked to the

decrease in fine detail. Moreover, when deviating a lot from the optimal distance  $V$ , the calibrating process becomes difficult. This is due to the calibration corner; this corner consists of a pattern that has to be covered by the projection and captured by the camera. When choosing a large process deviation it is difficult to achieve this and the calibration process may not be possible.

So in summary, it is not necessary to strictly adhere to the obtained equation of  $V$ . However, it is recommended to do this anyway, because this provides the highest level of detail and it assures that the calibration process can be executed.

### **6.3 Preliminary conclusion**

The findings in Section 6.2.1 makes it essential to make a modification in the setup. It has been found that it is necessary to have a situation where the scanning distance in the calibration setup is equal to the distance in the setup. Otherwise the scans are not reliable and thus useless. Therefore the optical distances from the scanning system to both the top and the bottom of the hand have to be exactly equal. This cannot be achieved with the current setup as described in Section 6.1, so an adaptation has to be made. Only when this is established, a feasible scanning system can be created. This will be the subject of Chapter 7.

*Note: The design so far is still 2D. This is done to minimize the complexity and to keep it uncluttered by omitting the unnecessary details. This is justified because the basic principles are the same for the 2D and the 3D situations. The advantage of this is that the experiments can be performed in a horizontal plane, because light beams are independent of gravity on this scale. The coupling to the 3D situation will be discussed later in this report and then this will be done with the knowledge obtained from the 2D analyses.*

## 7 Extended model

In the previous section it became clear that an adaptation is required to the total system in order to meet the requirements of Chapter 3. The solution is the addition of an extra mirror system above the projection surface. The use of this extra flat mirror system makes it possible to obtain same optical lengths for the top and the bottom side of the hand. As already motivated in Section 5.2, again two mirrors will be used in order to enable same incidence angles. The addition will not only change the top side of the entire optical system; it has also influence on the bottom side of the system. This chapter discusses the impact of these changes on the system and, as a consequence, describes the further elaboration of the total system.

### 7.1 Added mirror system

Previously a direct image of the top side of the hand was made. In the new situation the beams will be in contact with two mirrors before reaching the top side of the hand. The top mirror system in Figure 7.1 will be used to investigate the influence of the orientation of the mirrors.

In the figure the following parameters can be found:

- $\psi$ : the inclining angle of the first mirror with the vertical
- $\delta$ : the angle of incidence on the first mirror
- $\omega$ : the inclining angle of the second mirror with the vertical
- $\varepsilon$ : the angle of incidence on the second mirror
- $\alpha$ : the projection angle

The following relations can be found for the two angles of incidence:

$$\begin{aligned} \delta &= 180^\circ - \alpha - \psi \\ \varepsilon &= 180^\circ - (-\delta + \psi) - \omega \\ \varepsilon &= 180^\circ - (-180^\circ + \alpha + 2\psi) - \omega \\ \varepsilon &= 360^\circ - \alpha - 2\psi - \omega \end{aligned}$$

The same angle of incidence when:

$$\begin{aligned} \omega - \varepsilon &= \alpha \\ \omega - (360^\circ - \alpha - 2\psi - \omega) &= \alpha \\ 2\omega - 360^\circ + \alpha + 2\psi &= \alpha \\ \omega + \psi &= 180^\circ \end{aligned}$$

This implies that the same angle of incidence is obtained at the top side when the two mirrors are parallel to each other. Since the mirrors at the bottom side are also orientated as a result of this condition, the beams on the top and the bottom side of the hand have the same angle of incidence. This is one of the conditions required for the combination of the two images as discussed in Section 5.2. The other condition is that the optical distances from the scanning system to both the top and the bottom of the hand have to be exactly equal. As a consequence, the orientation of the mirror systems is already defined. However the position of the mirrors still needs to be determined. This will be elaborated in the next sections.

### 7.2 Position of the imaginary point sources

So far the orientations of the mirrors have been discussed. In Section 5.3 the orientation of the two mirrors below the hand and in Section 7.1 the orientation of the two mirrors on the top of the hand are discussed in Section 7.1. In this section the position of the mirrors will be discussed. The mirrors create imaginary point sources of the point sources in the scanning system, as a result of dual line reflections. The orientation and the (not yet obtained) position of the mirrors make it possible to determine the position of these imaginary point sources.

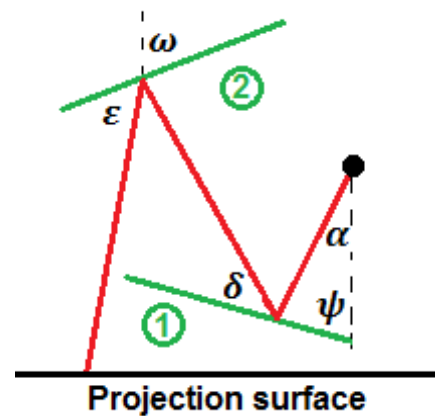
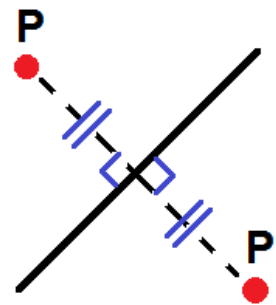


Figure 7.1 The top mirror system consisting of two mirrors

**7.2.1 Introduction**

For the determination of the position of the imaginary point sources use is made of the characteristics of reflection by a flat mirror. This states that the distance of a point P to the mirror is equal to the distance of the imaginary point P' to the mirror as illustrated in Figure 7.2.



**Figure 7.2** Reflection by a flat mirror

With this principle it is possible to calculate the position of the imaginary points created by the first mirror and using these points as input for the same principle on the second mirror one can obtain the position of the imaginary point sources of the scanning system.

**7.2.2 Determination of the coordinates for a given setup**

This principle as described in the previous section is elaborated in Appendix II. In the following, two systems will be introduced, namely a top system and a bottom system. The top system represents the mirror system above the hand and the bottom system represents the mirror system below the hand. The obtained equations for the coordinates of the imaginary point sources in Appendix II can be calculated with the use of the parameters shown in Figure 7.3 and 7.4

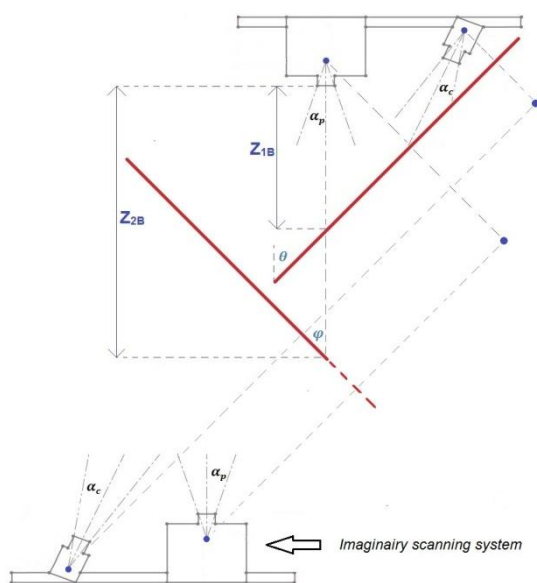


**Figure 7.3** The bottom mirror system with the imaginary scanning system caused by the two mirrors at a certain configuration

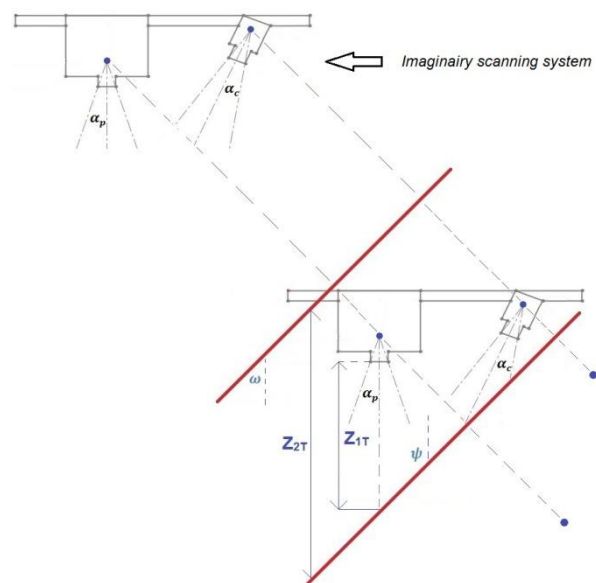


**Figure 7.4** The top mirror system with the imaginary scanning system caused by the two mirrors at a certain configuration

The equations of the coordinates of the imaginary scanning system contain the orientation ( $\theta, \varphi, \psi$  and  $\omega$ ) and the position with respect to the outside of the projector lens of the two mirrors for top and the bottom mirror system ( $Z_{1B}, Z_{2B}, Z_{1T}$  and  $Z_{2T}$ ) respectively. This enables the determination of the coordinates of the imaginary scanning system when the mirrors are fully defined. In Matlab [M5,M6] these calculations are elaborated for the two mirror systems, the coordinates of these imaginary scanning system can be determined for different mirror setups which fulfill the demand of a same angle of incidence, see Section 5.2 and 7.1. This results in coordinates of the imaginary scanning system which are orientated in a coordinate system of which the origin coincides with the projector point source. The equations for the coordinates of these imaginary point sources can be found in Appendix II.

By making use of the coordinates of the imaginary scanning system, it is also possible to know the location of the centre of the projection area. This is possible because it is known that the projection area is perpendicular to the vertical plane (and y-axis) and the scanning distance (E) is fixed at 650 mm, as discussed in Chapter 5.1. The coordinates of the top ( $x_{PCT}, y_{PCT}$ ) and the bottom ( $x_{PCB}, y_{PCB}$ ) projection plane become (see for clarification Figure 7.3 and 7.4):

$$\begin{aligned}x_{PCT} &= x_{PST} \\y_{PCT} &= y_{PST} - \left(E + (90 - SD_p)\right) \\ \\x_{PCB} &= x_{PSB} \\y_{PCB} &= y_{PSB} + \left(E + (90 - SD_p)\right)\end{aligned}$$

Here  $x_{PST}$ ,  $y_{PST}$ ,  $x_{PSB}$  and  $y_{PSB}$  represent respectively the coordinates of the imaginary projector point sources of the top and the bottom system, see Appendix II. Furthermore, the term  $(90 - SD_p)$  is the correction for the difference in distance between the projection point source and the outer lens (the scanning distance (E) is measured from the outer lens).

### 7.2.3 Coupling between the top and the bottom mirror system

In order to make a correct use of the two systems on both sides of the hand, the optical lengths to the top and the bottom side of the hand have to be equal. This enables a combining process of the two obtained scans as discussed in Section 6.3. Using this requirement makes it possible to combine the two mirror systems to one total mirror system and to further elaborate this system.

The condition of equal optical lengths requires that the centre of the two projection areas (the ones from the top and the bottom mirror system) coincides which each other, in other words that:

$$\begin{aligned}x_{PCT} &= x_{PCB} \\ &\text{and} \\ y_{PCT} &= y_{PCB}\end{aligned}$$

Making use of the obtained equations in Chapter 7.2.2 yields:

$$\begin{aligned}x_{PST} &= x_{PSB} \\ &\text{and} \\ y_{PST} &= y_{PSB} + 2\left(E + (90 - SD_p)\right)\end{aligned}$$

Looking at the equations for  $x_{PST}$ ,  $y_{PST}$ ,  $x_{PSB}$  and  $y_{PSB}$  in Appendix II leads to the conclusion that this results in two equations with eight unknowns ( $\theta, \varphi, \psi, \omega$  and  $Z_{1B}, Z_{2B}, Z_{1T}, Z_{2T}$ ). To be more precise, Chapters 5.2 and 7.2 showed that there are actually six unknowns left because of the relations that exist between the inclining angles  $\theta, \varphi$  and  $\psi, \omega$ . However, this results in still too much unknowns to solve the system. Therefore the characteristics of the resulting unknowns will be investigated in the following sections. This is done to be able to adapt simplifications to the system at a later time and hereby reduce the number of unknowns and enabling the solving of the equations.

### 7.3 Tests with the adapted model

In this section the characteristics of the bottom and the top mirror system will be investigated. There is looked at the influence of the mirror location and the inclining angles. These analyzes are done using the obtained coordinates of the top and bottom mirror systems (see Appendix II). Using these findings makes it possible to combine these two systems and to solve the equations in Section 7.2.3.

### 7.3.1 Characteristics of the bottom mirror system

The operations in this section have been executed with Matlab [M7,M8]

During the variation of the location of the bottom mirrors three different situations have been considered: a situation where  $Z_{1B}$  is varied, a situation where  $Z_{2B}$  is varied and a situation where  $Z_{1B}$  is equal to  $Z_{2B}$ . So in other words, at two situations where the inclining point of the two mirrors are at different locations and one situation where these points collapse. The effects of these operations on the coordinates of the imaginary projector point sources are shown in the figures below.

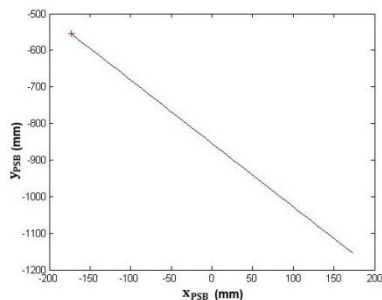


**Figure 7.5** Effect of variation of  $Z_{1B}$  on  $x_{PSB}$  and  $y_{PSB}$

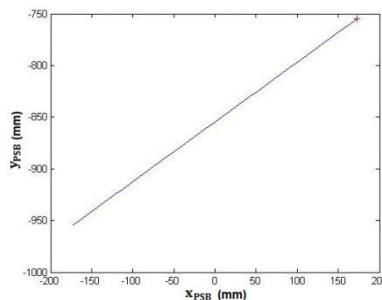


**Figure 7.6** Effect of variation of  $Z_{2B}$  on  $x_{PSB}$  and  $y_{PSB}$

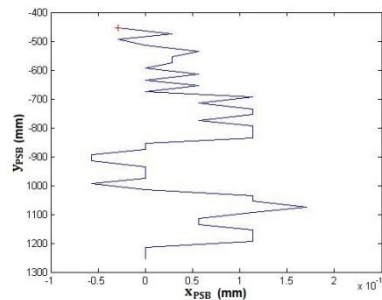


**Figure 7.7** Effect of variation of  $Z_{1B} = Z_{2B}$  on  $x_{PSB}$  and  $y_{PSB}$

Looking at the three figures, the following can be noticed. When  $Z_{1B}$  or  $Z_{2B}$  is varied while the other mirror stays at its location, the location of the imaginary projector point source varies linearly. Both the x-coordinate as the y-coordinate changes. When  $Z_{1B}$  is chosen equal to  $Z_{2B}$  and the mirrors are moved vertically simultaneously; only the y-coordinate changes (the variation of the x-coordinate is due to numerical errors, furthermore it is in the order of  $10^{-13}$  mm and therefore negligible).

During the variation of the inclining angles three different situations are relevant: a situation where  $Z_{1B}$  is larger than  $Z_{2B}$ , a situation where  $Z_{1B}$  is smaller than  $Z_{2B}$  and a situation where  $Z_{1B}$  is equal to  $Z_{2B}$ . The angles are varied according to the boundary equations obtained in Section 5.3. So in other words, the angle between the two mirrors is equal to  $90^\circ$ , while this total angle can be rotated in space. The results of these operations in terms of the coordinates of the imaginary projector point sources ( $x_{PSB}$  and  $y_{PSB}$ ) are shown in the figures below.

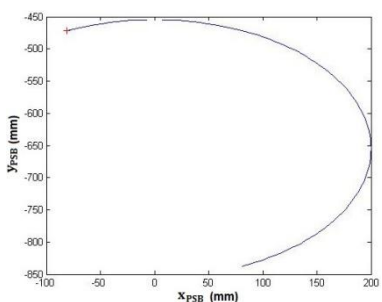


**Figure 7.8** Effect when  $Z_{1B}$  is larger than  $Z_{2B}$

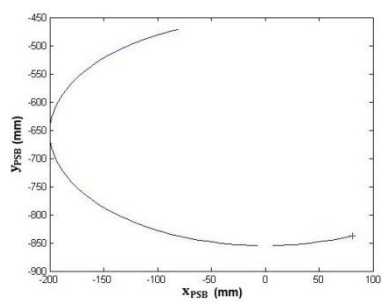


**Figure 7.9** Effect when  $Z_{1B}$  is smaller than  $Z_{2B}$

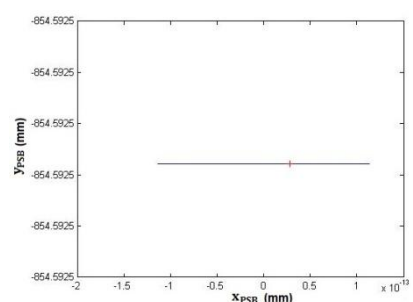


**Figure 7.10** Effect when  $Z_{1B}$  is equal to  $Z_{2B}$

Looking at these three figures, the following can be noticed. When  $Z_{1B}$  is not equal to  $Z_{2B}$ , the location of the imaginary projector point source varies a lot. Both the x-coordinate as the y-coordinate changes. For situations where  $Z_{1B}$  is chosen equal to  $Z_{2B}$  the location of the imaginary projector point sources is kept constant for different orientations (neglecting numerical errors). This means that when  $Z_{1B}$  is chosen equal to  $Z_{2B}$  (so the position of the inclining points are the same and are vertical with the projector) the location of the imaginary projector point source is vertical

with the projector. This means that it is independent of the total orientation of the mirrors. This property is desirable because an eventual small deviation in the total orientation of these two mirrors will have no influence on the performance of the scanning system.

This correctness of this statement is checked with a setup where the two mirrors are inclined directly below the projector ( $Z_{1B}$  is equal to  $Z_{2B}$ ) and the angle between these mirrors is  $90^\circ$ . For this basic setup three different situations are created where the total orientation of these two mirrors is varied each time. From these three situations scans are made of a wooden rod. These different scans are combined in a same coordinate system with different colours in Figure 7.11 and 7.12.

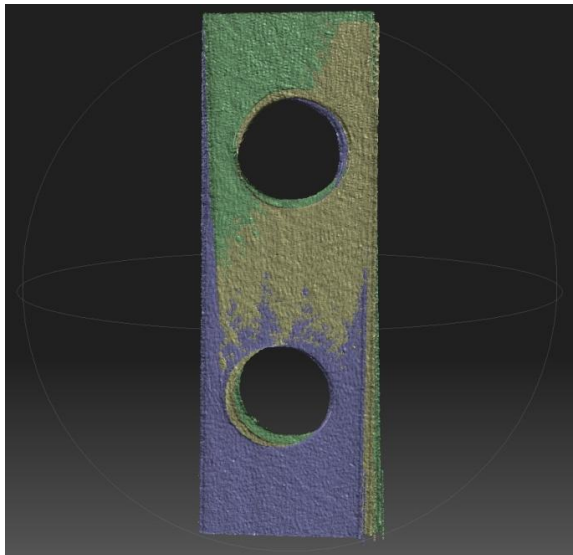


Figure 7.11 Front view of the combined scans

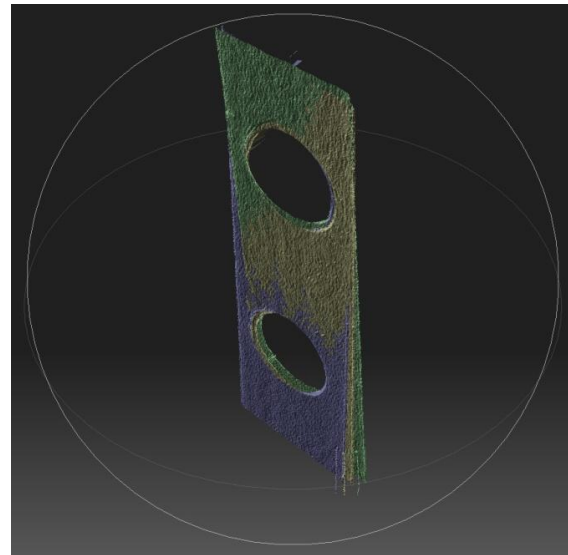


Figure 7.12 Side view of the combined scans

These figures show that the three rods overlap pretty well. The errors are caused by inaccuracies of the setup; this will be discussed later. But the main goal is achieved and the feasibility is proven.

### 7.3.2 Characteristics of the top mirror system

*The operations in this section have been executed with Matlab [M9,M10]*

During the variation of the location of the top mirrors three different situations three different situations are relevant: a situation where the location of the first mirror is varied, a situation where the location of the second mirror is varied and a situation where the locations of the two mirrors are changed simultaneously while the distance between the mirrors remain the same ( $Z_{2T}$  is constant). The results of these operations in terms of the coordinates of the imaginary projector point sources ( $x_{PST}$  and  $y_{PST}$ ) are shown in the figures below.

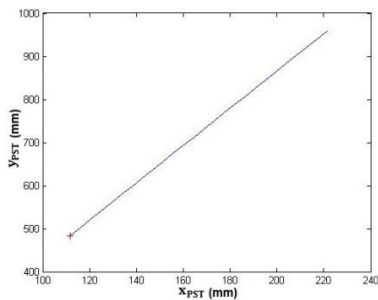


Figure 7.13 Variation of the first mirror position

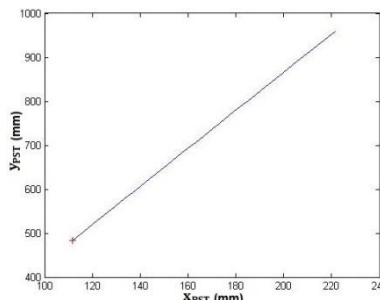


Figure 7.14 Variation of the second mirror position

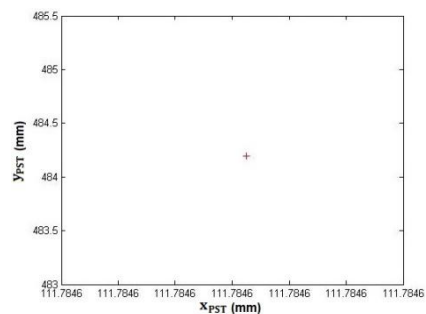
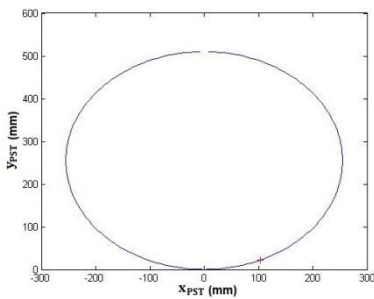


Figure 7.15 Variation of the mirror positions ( $Z_{2T}$  is constant)

The variations of the two mirrors in the first and second situation are applied in the same way, the step sizes are equal such that  $Z_{2T}$  varies in the same way. Looking at the three figures, the following can be noticed. The results of the first two situations, Figure 7.13 and 7.14, are equal to each other. This would mean that the position of the imaginary projector point source is only depending on  $Z_{2T}$  and independent of the mutual position of the two mirrors, thus  $Z_{1T}$ . This is confirmed by Figure 7.15, where different mirror positions with a same  $Z_{2T}$  result in the same coordinates of the imaginary projector point source (given by the red cross). This would also mean that the obtained equations for  $x_{PST}$  and  $y_{PST}$  have to be independent of  $Z_{1T}$ ; this is checked and elaborated in Appendix III.

During the variation of the inclining angles there is looked at three different situations. The difference between the first two situations is the difference in the mirror locations while  $Z_{2T}$  is kept constant and the third situation is a case where a variation in  $Z_{2T}$  is applied. During these three situations the two inclining angles are varied according to the findings in Section 7.1. The results of these operations in terms of the coordinates of the imaginary projector point sources ( $x_{PST}$  and  $y_{PST}$ ) are shown in the figures below.



**Figure 7.16** First mirror position with a certain  $Z_{2B}$

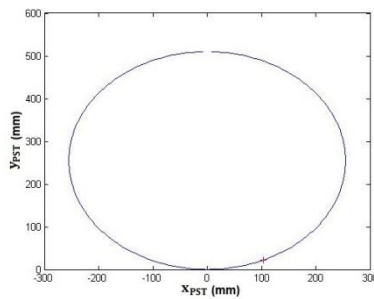


**Figure 7.17** Second mirror position with the same  $Z_{2B}$

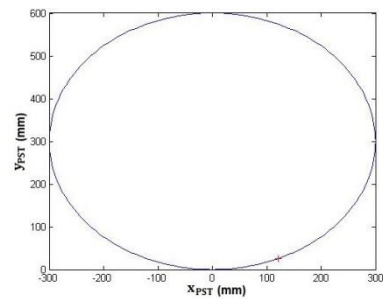


**Figure 7.18** Mirror position using a different  $Z_{2B}$ .

The figures confirm that the coordinates are only depending on  $Z_{2T}$  and are independent of  $Z_{1T}$ . Because Figure 7.16 and 7.17 are the same and the results change for different  $Z_{2T}$  (Figure 7.18).

### 7.3.3 Combining the two mirror systems

In Sections 7.3.1 and 7.3.2 the characteristics of both mirror systems are investigated, this resulted in the following conclusions:

$$Z_{1B} = Z_{2B}$$

$\theta, \varphi$  are freely selectable (no influence)

$Z_{1T}$  is freely selectable (no influence)

These conclusions reduce the amount of depending variables in the system to four:  $Z_{2T}$ ,  $Z_{2B}$ ,  $\psi$  and  $\omega$ . The variables  $\theta$  and  $\varphi$  became freely selectable with the boundary condition that  $Z_{1B} = Z_{2B}$ , the results of this condition was that the position of the imaginary projector point source was vertical with the original projector point source (see Section 7.3.1). This has also consequences for the inclining angles of the mirrors in the top mirror system. Namely, this leads to the restriction that these mirrors have to be horizontal, which means that  $\psi = \omega = 90^\circ$ . This reduces the depending variables to two; only  $Z_{2T}$  and  $Z_{2B}$  will influence the position of the imaginary projector point sources.

The obtained set of equations in Chapter 7.2.3 is also influenced by this. The first equation cancels out so that only one equation is left over; this equation will be called the coupling equation from now on:

$$y_{PST} = y_{PSB} + 2(E + (90 - SD_p))$$

This means that when one of the two depending variables is chosen ( $Z_{2T}$  or  $Z_{2B}$ ) the remaining variable is automatically determined with the use of this equation so that the two mirror systems can be combined. When this is achieved, the combining process of the two scans (bottom and top side of the hand) is also automatically executable. The findings so far are summarized in Table 7.1 below; the values in this table will be used in the remainder of this report. In addition, two new variables ( $Z_T$  and  $Z_B$ ) are introduced in order to replace the existing variables to avoid confusion. This all is illustrated in Figure 7.19, where an overview of the total system is shown.

Parameter	Value
$\theta$	$45^\circ$ (*)
$\varphi$	$45^\circ$ (*)
$Z_{1B}$	$Z_{2B}$
$Z_{2B}$	$Z_B$
$\psi$	$90^\circ$
$\omega$	$90^\circ$
$Z_{1T}$	freely selectable (**)
$Z_{2T}$	$Z_T$
$\alpha_p$	$12.2969^\circ$
$\alpha_c$	$11.2667^\circ$
$SD_p$	$62.7038 \text{ mm}$
$SD_c$	$26.8233 \text{ mm}$
$E$	$650 \text{ mm}$ (***)
$V$	$230.7143 \text{ mm}$
$\lambda$	$72.6838^\circ$

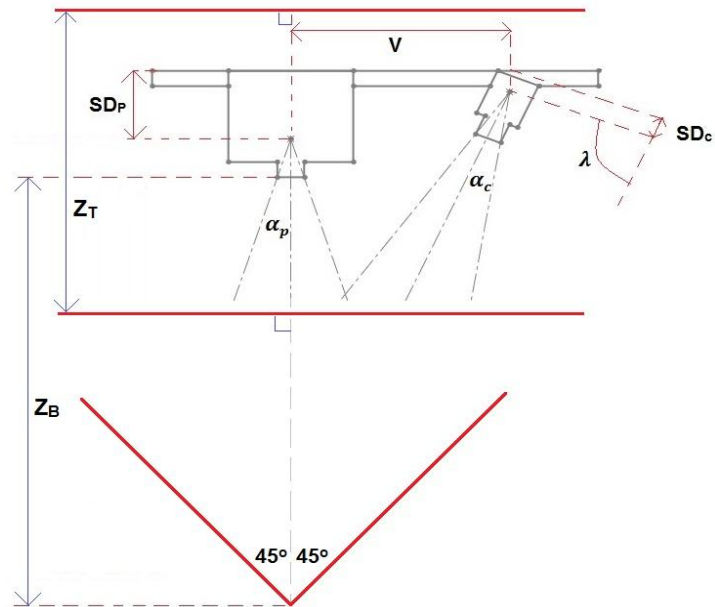


**Table 7.1** Overview of the parameters **Figure 7.19** Overview of the total system

The inclining angles of the two mirrors in the bottom system were freely selectable, but to reduce the complexity this values are set to  $45^\circ$  (see table x \*). In Section 7.3.2 it is shown that the position of the projection area is independent of  $Z_{1B}$ . This is true, but this value must be chosen such that it does not lead to geometric problems (see table x \*\*); this will be treated in Chapter 9. In Section 5.1 the scanning distance  $E$  is set to  $650 \text{ mm}$  (see table x \*\*\*), therefore the parameters  $V$  and  $\lambda$  are also determined (see Sections 4.6 and 5.5). Choosing  $Z_T$  and  $Z_B$  according the obtained coupling equation enables that the optical length of the bottom and that of the top system are equal. This ensures that the two scans can be combined. Note that in Figure 7.19 the first mirror of the top system blocks the pattern for the bottom mirrors; a solution for this problem will be given in Chapter 9.

### 7.3.4 Conforming the correctness of the total system

To investigate the feasibility of this optical system three different scans made of the wooden rod (already treated in Section 7.3.1) will be combined:

- A scan without mirrors at a scanning distance of  $650 \text{ mm}$  ( $E$ )
- A scan using only the top mirror system with a certain distance  $Z_T$
- A scan using only the bottom mirror system using a certain distance  $Z_B$

The reliability of the system will be tested by choosing values of  $Z_T$  and  $Z_B$  such that the coupling equation in Section 7.3.3 is fulfilled and the optical lengths of the two systems are equal to  $650 \text{ mm}$ . The coupling equation can be further elaborated with the use of the reduced equations for the coordinates of the imaginary projector point sources, this is elaborated in Appendix IV. This results in the following equations for the coordinates  $x_{PSB}$ ,  $y_{PSB}$ ,  $x_{PST}$  and  $y_{PST}$  :

$$\begin{aligned}
 x_{PSB} &= 0 & x_{PST} &= 0 \\
 y_{PSB} &= -2 \left( Z_B + (90 - SD_p) \right) & y_{PST} &= 2Z_T
 \end{aligned}$$

This reduces the coupling equation of Section 7.3.3 as follows:

$$y_{PST} = y_{PSB} + 2(E + (90 - SD_p))$$

$$2Z_T = -2(Z_B + (90 - SD_p)) + 2(E + (90 - SD_p))$$

$$Z_T + Z_B = E$$

There is chosen to set the distance  $Z_T$  to 225 mm (and  $Z_{1T}$  to 40 mm), filling this value for  $Z_T$  in the reduced coupling equation gives [M11]:

$$Z_B = E - Z_T = 650 \text{ mm} - 225 \text{ mm} = 425 \text{ mm}$$

Now these values are determined, the three setups can be built and the scans can be made. The results of these scans are combined in an equal coordinate system in Figure 7.20 and 7.21 below:

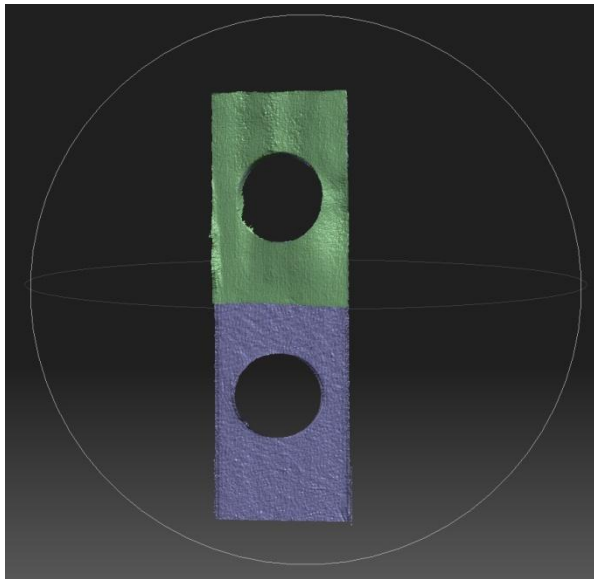


**Figure 7.20** Combining the scans of the bottom mirror system (blue) and the top system (green)

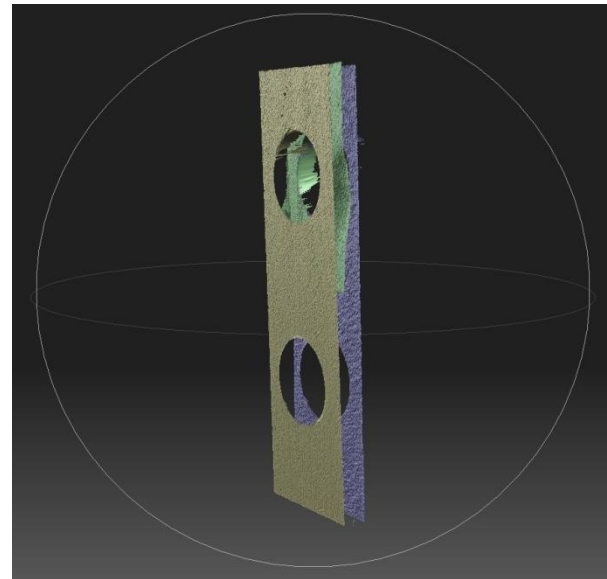


**Figure 7.21** All three scans; direct scan (brown), bottom scan (blue) and top system (green)

The first impression of Figure 7.20 and 7.21 is that these scans overlap pretty well. Figure 7.20 shows that the bottom and the top system are well matched, Figure 7.21 shows a little deviation in the depth. This leads to the conclusion that the frontal views of the scans are comparable in a great extent, but that the optical lengths differ reciprocally. This variation in the optical lengths is caused by the thickness of the mirrors which is not taken into account in the design so far. The reader may note that the scan from the bottom system does not contain the full image of the wooden rod, this is caused by a geometric restriction that also will be discussed in Chapter 9.

#### 7.4 Discussion

In this chapter the system has been extended with a second mirror system. The two resulting mirror systems, the new one on the top side of the hand and the existing on the bottom side, were combined to one total optical system with the use of the coupling equation which is based on equal optical lengths. The working principles of the total system were discussed and the feasibility of the total system is demonstrated. Several additional problems have to be further elaborated, but the overall conclusion is that the scans from the two mirror systems are comparable and this means that the chosen design of the total system is justified!

*Besides the Matlab Scripts that are designed for this chapter, also Solidworks Models are made that give a visualization of the total optical system setup [S1,S2].*

## 8 Combining algorithm

In the previous chapter the working of the total optical system is elaborated. Now the working principle of the system is known, the next step can be investigated. This is the combining process of the two scans of the top and the bottom side of the hand into one image of the total hand. In order to be able to do this one has to know the position and the orientation of these images of the hand. Therefore the location of the images has to be known expressed in the coordinate system belonging to the DAVID software. However, the research and results so far are done and expressed in a global 2D coordinate system where the point source of the projector is the centre of it. Therefore in order to make the equations compatible, a transformation to the other coordinate system is needed.

### 8.1 Characteristics of the coordinate system of DAVID

In the DAVID software the coordinate system is based on the view range of the camera. Several measurements showed that the coordinate system is proportional to the view on the laptop display when performing a scan. This means that two axes are parallel to the lens of the camera and the third one is perpendicular to this lens. Besides that the centre of the captured image on the laptop is the centre of the coordinate system. This is illustrated in Figure 8.1.

In this figure the black line represents the projection area. The orientation of the camera is such that the centre of the camera range intersects with the centre of the projection area (Section 5.5). This intersection point is the centre of the red coordinate system of the camera.

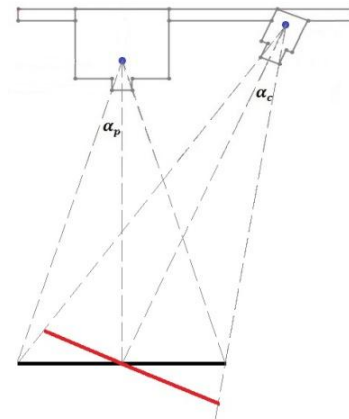


**Figure 8.1** The coordinate system of the scanning system

The scans that are made and exported with the DAVID software have the file extension OBJ. The OBJ file format is a simple data-format that represents 3D geometry in terms of the position of each vertex. The advantage of this file format is that it is open source and that it has been adopted by other 3D graphics application vendors (like Matlab). This makes it possible to make adaptations in the images of the scans when the setup of the file is understood.

An OBJ file contains several types of definitions, below an example of an OBJ file format is shown:

```
-----
# Mesh file generated with DAVID-Laserscanner version 3
# Simon Winkelbach and Sven Molkenstruck
# www.david-3d.com

# List of vertices with (x,y,z) coordinates:
v -25.406710 90.830520 58.189400
v -25.579740 90.825020 58.344980
v -25.399060 91.064790 58.192390
.....
# x vertices

# List of triangles:
f 1 3 2
f 3 1 4
f 5 4 1
.....
# y triangles
-----
```

Such a file format contains three kinds of information: the first paragraph contains information about the program that created the file, the second paragraph contains the coordinates of all the vertices and the last paragraph contains information about the triangles (faces in the mesh). The second and third paragraphs have the same kind of setup. In the paragraph of the vertices each line contains a 'v' that stands for vertex and is followed by three numbers that represent the coordinates of the vertex (respectively x, y and z). In the paragraph of the faces each line contains an 'f' that stands for face and is followed by three numbers. Each number 'n' refers to a single vertex, the n<sup>th</sup> vertex in the second paragraph. In this way a face is defined by three vertices. The length of the second and third paragraphs depends on the number of vertices (x) and faces (y).

## 8.2 Working with the OBJ file format

The OBJ file format can be opened in Matlab to change and manipulate the codes of the vertices and faces, in this way the images of the scans can be changed. The problem is that the scans from DAVID contain a lot of details and therefore the codes cannot be directly edited in Matlab because this asks too much effort from Matlab (leading to the error: 'there is not enough memory to open the file in the editor'). However, the codes can be manipulated in the background of the program, but the codes cannot be seen during these operations.

A solution for this problem is the program Meshlab. Meshlab can minimize the number of faces to an exact value and thus reducing the memory needed in Matlab (and other programs). This operation is described in the Bachelor-Thesis of Marcel Heinric [2]. Successfully completing this operation makes the object itself appears more coarse, but at the same time maintaining a sufficient level of detail. Another consequence of this operation is that the contents of the OBJ file format changes. Obviously is that the number of vertices and faces are reduced, so that the length of the format is reduced. But the file format as described in Section 8.1 is also affected; the new format is as follows:

```
-----
####
#
# OBJ File Generated by Meshlab
#
####
# Object TestMiddelpuntLinks_heelklein.obj
#
# Vertices: x
# Faces: y
#
####
vn 1.554683 -0.064627 1.810642
v -18.939816 89.613838 52.739632 0.749020 0.749020 0.749020
vn 1.841371 -0.077241 2.148877
v -7.136764 90.378662 42.637894 0.749020 0.749020 0.749020
vn 2.136679 -0.091644 2.492276
v 4.638305 88.520111 32.505199 0.749020 0.749020 0.749020
vn 1.320260 -0.054856 1.537756
.....
# x vertices, 0 vertices normals

f 7//7 1//1 4//4
f 1//1 7//7 5//5
f 5//5 9//9 2//2
f 9//9 11//11 2//2
# y faces, 0 coords texture

# End of File
-----
```

This file format contains, except for the same information, also extra (new) information. The three paragraphs from Section 8.1 are still recognizable, but the content is changed. The first paragraph shows that the file is adapted by Meshlab ('OBJ File Generated by Meshlab') and includes more lines than in the previous case. The paragraph with the vertices contains new lines, these lines starts with 'vn' followed by three numbers. These lines represent the normal coordinates. What is striking too is that the 'v' lines are expanded with three extra numbers; these numbers represent the weighting factors. The lines which contain information about the faces (third paragraph) are also affected; the original three numbers are replaced by three terms with two numbers divided by a backslash. These terms are the vertex number followed by the normal index values.

It can be concluded that the contents of this new file format has a lot of resemblance with the old one, but is more extensive. All this extra information is superfluous and makes the file format unnecessary complex. But the advantage is that this new format can now be directly edited by Matlab and the computation time is reduced because of the smaller file format. This means that the user has two options:

- Editing the OBJ file generated by DAVID on the background of Matlab without direct control because the operations are not visible during the process.
- Editing the OBJ file generated by Meshlab which takes less computation time but includes an unnecessary complex file format.

The second option is the preferred one, but therefore the complex file format has to be simplified to a file format similar to the clear one generated by DAVID. Further analyzing of the complex format showed that the lines with the normal indices ('vn lines') can be deleted without consequences. These deleting operations give no problems with lines which contain information about the faces ('f lines'); these act just as the original 'f lines' in Section 8.1. This means that the complex OBJ files generated by Meshlab can be easily compiled back to the clear format of the OBJ files of DAVID. The contents of these file formats will be used as basis for the manipulation software in the next section.

### 8.3 Simulating the manipulation of the points

The advantage of the discussed file format is that the faces of the body are only based on the vertices themselves and not on the position of these vertices. This means that for rotations and translations of the image only the 'v lines' have to be adjusted and the 'f lines' can remain unmodified. The combining process of the top image and the bottom image of the hand requires that the position of these images with respect to the rotational axes are known. For the 2D situation that has been discussed in Section 7, there is only one rotational axis through the centre of the coordinate system and the rotation angle between the two images is equal to  $90^\circ$  (see Figure 5.1 in Section 5.1 and Figure 7.19 in Section 7.3.3). This leaves a theoretically simple situation with just one mirror line.

However, for situations where this property is not valid (due to imperfections in the total system or other designing choices), the properties of the mirror line and location of the rotation point have to be determined. In the following a solution is given for these complex cases, this is carried out to the situation illustrated in Figure 8.2 and 8.3.

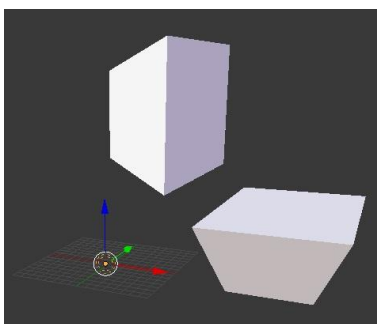


Figure 8.2 A 3D body that needs to be mirrored

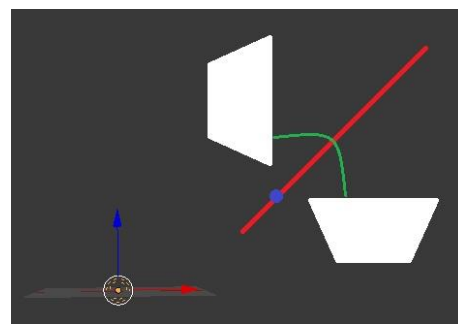


Figure 8.3 The properties needed for rotation

In Figure 8.2 a random orientated 3D body (random3dbody.obj) is shown that needs to be mirrored with its mirror image to gain the full 3D image (the left body is in the correct position and the right body needs to be rotated). This becomes possible when the properties illustrated in Figure 8.3 are obtained: the mirror line (red), the rotation point (blue) and the total rotation angle (green). For this kind of situations a Matlab script is developed that provides these three properties [M12]. In this script also a correction for the coordinate system is included: this is needed because Blender (software that is introduced in the Bachelor-Thesis of Marcel Heinric [2]) uses a (x,z,-y)- coordinate system instead of the generalized (x,y,z)-coordinate system that is present in the OBJ file format. Note that this script uses corresponding points on the two bodies to generalize the desired properties. In this script use is made of extreme coordinate values, in case this method is not applicable for a different situation, then markers or the like will have to be used.

When these properties are determined the rotation can be performed. This operation is done using a rotation matrix and a generalized coordinate system from which its centre coincides with the rotation point. This rotation is performed in Matlab [M13]. This script provides new vertices for the mirrored 3D body in such a way that it attaches to the other body (where a conversion is done again to the other coordinate system). When these obtained vertices (new 'v lines') are substituted for the 'v lines' in the original OBJ file this results in a full 3D image. This is done with rotated3dbody.obj and this result is illustrated in Figure 8.4. In this figure the rotation of the mirrored part of Figure 8.2 is shown.

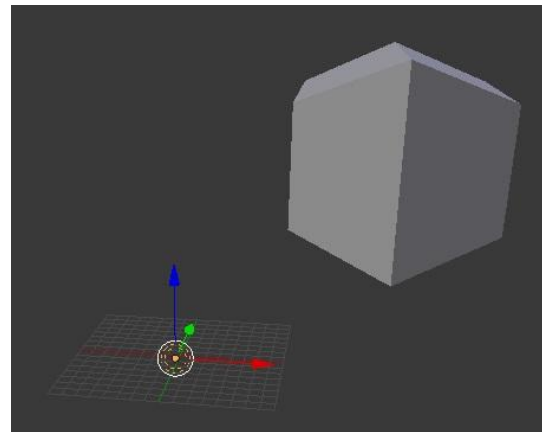


Figure 8.4 Mirrored 3D image of the body

#### 8.4 Application on the scanning system

The operations explained in Section 8.3 can be applied to the designed scanning system in Chapter 7. For this situation it is known that the rotation angle is equal to  $90^\circ$  and the rotation point coincides with the centre of the coordinate system (see Figure 8.1 in Section 8.1). But because the plane on which the scanning system is focused determines the location of the coordinate system, it is investigated what the consequences are for the rotation process as described in Section 8.3. This is done using a Matlab scripts [M12,M13] where all the operations described in Section 8.3 are combined and the OBJ file format is automatically updated to the correct (new obtained) vertices. Two situations are investigated; the first one is a situation where the scanning system is focused on the top side of the hand and in the second situation the focus is on the bottom side of the hand. During these operations a simulation of the hand is made as shown in Figure 8.5 and 8.6. These images are created using the requirement of equal optical length and according to the reduced coupling equation of Section 7.3.4. For convenience it is also assumed that the camera view is perpendicular to the hand; this simplifies the properties of the coordinate system.

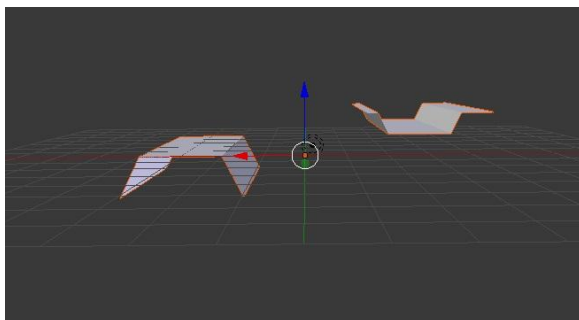


Figure 8.5 Focus on the top side of the hand

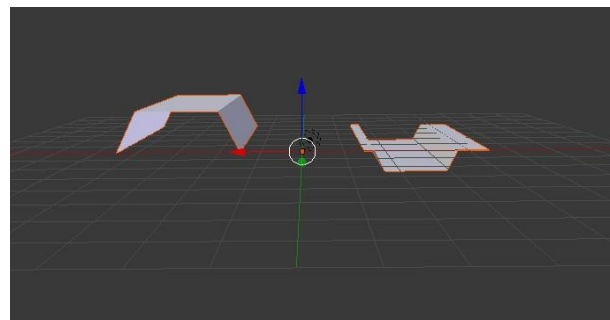
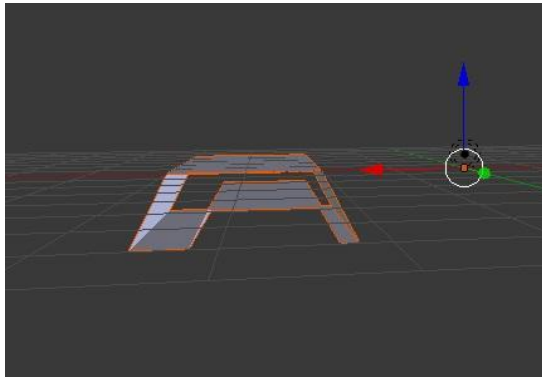
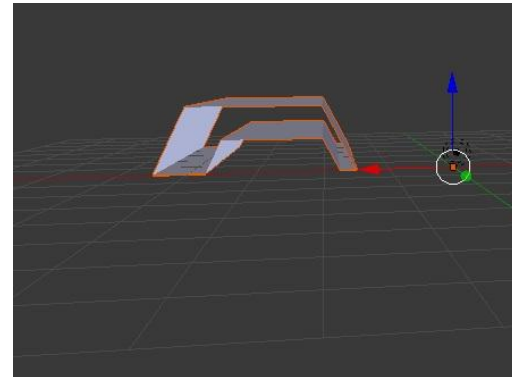


Figure 8.6 Focus on the bottom side of the hand

The rotations needed for the two situations are executed in two different Matlab scripts; these are 'Rotation\_focus\_top.m' [M14] for the situation in Figure 8.5 and 'Rotation\_focus\_bottom.m' [M15] in Figure 8.6. These operations result in the formation of two OBJ file formats which contain the data for the mirrored hand image, respectively 'Hand\_result\_top.obj' and 'Hand\_result\_bottom.obj'. The results are shown respectively in Figure 8.7 and 8.8.



**Figure 8.7** Focus on the top side of the hand



**Figure 8.8** Focus on the bottom side of the hand

Figure 8.7 and 8.8 show that the top and the bottom side of the hand are attached to each other and thus both operations are executed correctly (the space between the top and the bottom side of the hand is simulated deliberately in order to approximate the actual reality).

## 8.5 Discussion

This chapter shows that it is possible to rotate a part of a body on/to another part of the same body. Those operations are executed with the discussed Matlab scripts. In order to rotate two bodies, the plane on which the scanning system is focused has to be determined. Because the system has to be operated for different patients (and thus different hand thicknesses), the scanning system has to be focused on a fixed object where the patient is laying down his hand. This means that the situation where the focus is on the top side of the hand in the previous section is not practicable.

In order to rotate other mirrored bodies, Matlab script 'Combining\_algorithm.m' [M16] has been created. This script enables the rotation of random mirrored bodies when the following conditions are fulfilled:

- The two parts of the body are related to each other by just one mirror line, not more. This means that there exists only one rotation angle in one plane.
- Corresponding points on the two parts are obligatory; this can be achieved by geometry or markers or the like.
- The two sets of vertices of the two parts have to be separated or at least it has to be known if a vertex belongs to the top side or bottom side of the object.

When the system is installed as prescribed in Section 7.3.3, the rotation angle is equal to  $180^\circ$  and the rotation point is coinciding with the centre of the coordinate system. This is a favorable property and therefore the system has to be set up and calibrated precisely because little variations lead to incorrect functioning of the rotation process. Moreover, the system must be designed rigid in order to retain this property.

## 9 Elaboration of the theoretical model

In this chapter the focus is at certain pre-determined orientations of the mirrors as discussed in Section 7.3.3. The use of the reduced coupling equation (see Section 7.3.4) assures that the scanning distance of the two mirror systems is equal to  $D_{min}$  and thus that the optical lengths for both scans are equal. Using this property makes it possible to determine both the position and the optical range of the imaginary point sources of the scanning system which are created by the two mirror systems. The theoretical model from Chapter 7 will be elaborated and a primitive prototype will be realized.

### 9.1 Realizing the coupling

In Section 7.3.3 the complication of the blocking of the beams by the mirrors was introduced; this will be explained now using Figure 9.1. The camera and the projector beam from the scanning system have to reach the mirrors of the bottom system (mirrors 3 and 4), while at the same time they also have to reach the mirrors of the top system (mirrors 1 and 2). This means that mirror 1 has two functions: transmission of the beams towards mirrors 3 and 4 and reflection of the beams towards mirror 2.

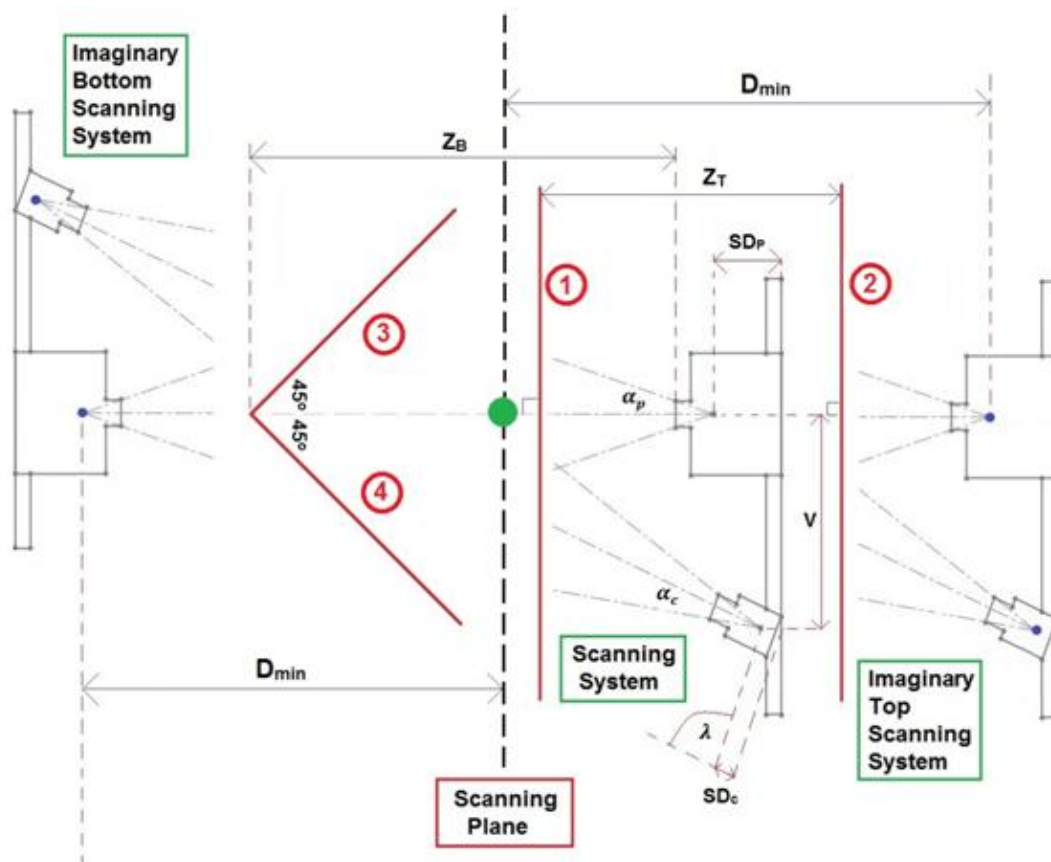


**Figure 9.1** Overview of the total system with the imaginary scanning systems

One half of the range of the beams has to be used for the top system and the other half has to be used for the bottom system in order to enable the combination of the two images. This property can be achieved in case mirror 1 is splitted in a set of two mirrors which only reflect one half of the beam range of the projector and the camera, while the remainder of the light hits mirrors 3 and 4, as illustrated by the markers 'B' and 'T' in Figure 9.2. This makes the separated mirrors at mirror 1 important factors of the setup because their sizes have to be adjusted such that this behavior is realized. When these mirrors can fulfill this condition, the centre of the coordinate system (marked with a green circle) will be the boundary between the two images. Furthermore, the inner edges of the beams from the two imaginary scanning systems will go exactly through this point, such that the images of the top and the bottom side of the hand can be combined as discussed in Section 8.5.

For the other mirrors in the setup there is no certain geometry restriction, they only have to be large enough to reflect all the light of the incoming beams. Therefore only attention will be paid to the sizes of the two mirrors at mirror position 1.

**9.2 Determination of the mirror sizes**

In the previous section the importance of the two separated mirrors at position 1 has been discussed. The intended working of these mirrors will be illustrated with Figure 9.2.

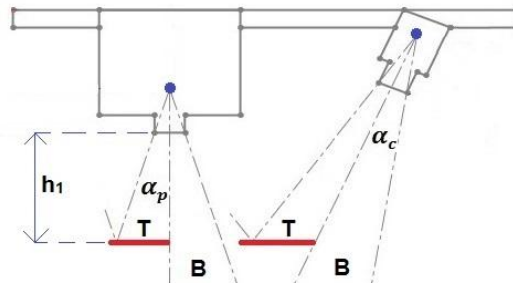


**Figure 9.2** Intended mirror setup at mirror position 1 such that the beams are splitted in half

In this figure it can be seen that the mirrors have to be big enough to reflect the half of the beams to the top mirror system (T), but they also have to be not too big to make sure that the other half of the beams can pass to the bottom mirror system (B). Therefore it is important that the mirrors are installed exactly with their mirror edges on the bisector of both beams. A maximum value for  $h_1$  can be determined using the fact that the total scanning distance has to be equal to 650 mm (E). A minimum value for  $h_1$  can be determined using the fact that the reflection of the projector has to pass over the height of the projector to the second mirror. This is investigated in Appendix V; the results for these two values are:

$$h_{1max} = 140.0000 \text{ mm}$$

$$h_{1min} = 295.4376 \text{ mm}$$

Comparing the values of  $h_{1min}$  and  $h_{1max}$  results in the conclusion that such a solution is physically impossible because  $h_{1min}$  is larger than  $h_{1max}$ . Therefore the whole scanning system needs to be tilted vertically in order to overcome the height of the projector and thus to reduce the value of  $h_{1min}$ . This gives the mirror system an extra degree of freedom as illustrated in Figure 9.3.

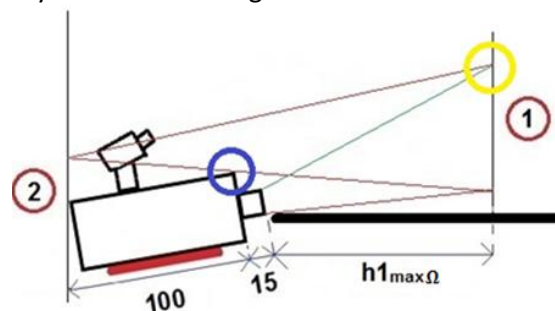


**Figure 9.3** Top mirror system with the minimum vertical tilt angle  $\Omega$  and two boundary conditions (yellow and blue circles), dimensions are in mm.

In this figure it is assumed that the bottom side of the lens is against the edge of a horizontal surface. Further investigation showed that there are two boundary conditions, these are shown in the figure. The first requirement is that the position at the first mirror of the second mirror reflection of the lowest ray is higher than that of the highest projection ray. In this case the mirror at position 1 is high enough to reflect the whole range of the projection and simultaneously does not block the intended reflections. This boundary condition is encircled yellow in Figure 9.3. The second requirement is that the lowest projection ray, after reflection at the first mirror, is not blocked by the projector and it is able to pass the projector unhindered. This boundary condition is encircled blue in the figure.

To calculate the minimum tilt angle  $\Omega$  that is needed to fulfill both boundary conditions, the distance  $h_1$  needs to be specified. This minimum required angle decreases with increasing distance  $h_1$ . A larger tilt angle induces an image of the hand containing less detail, as concluded in Section 6.2.2; therefore it is assumed that a maximum tilt angle of  $20^\circ$  is permitted. This assumption leads to a maximum mirror distance  $h_{1\max\Omega}$ , this is further elaborated in Appendix VI. With this maximum distance it is possible to calculate the minimum tilt angles for the two discussed situations; this is done in Matlab [M18].

Matlab calculated a minimum tilt angle of  $3.8515^\circ$  with a maximum mirror distance ( $h_{1\max\Omega}$ ) of  $125.8623\text{ mm}$  (explanation of this elaboration in Matlab can be found in Appendix VI). Besides that, a Solidworks file is generated to provide more insight in the rotated scanning system [S3].

Using this minimum vertical tilt angle  $\Omega$  and the intersection points of the projector and camera rays on the first mirrors makes it possible to calculate the maximum mirror dimensions, as is illustrated in Figure 9.4. These calculations are again performed in Matlab [M18]. Because the two mirrors will be inclined on the same plane (see next section), the heights of the projector mirror ( $h_{mp}$ ) and that of the camera mirror ( $h_{mc}$ ) are defined from this same plane. Explanation of this process can be found in Appendix VI.

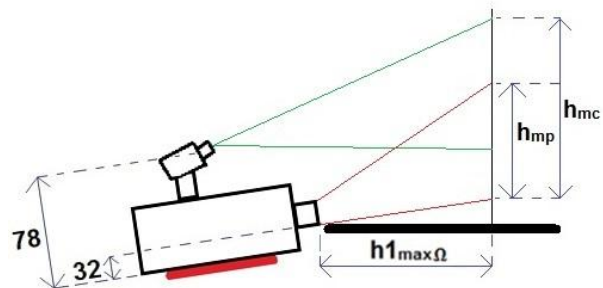


**Figure 9.4** Reflection points at the first mirror with the heights of the two mirrors  $h_{mp}$  and  $h_{mc}$ .

The calculations in Matlab [M18] resulted in the following two mirror sizes (width x height):

Size of projector mirror:  $33.3853\text{ mm} \times 54.2991\text{ mm}$   
 Size of camera mirror:  $44.3398\text{ mm} \times 98.5687\text{ mm}$

### 9.3 Design of the prototype

Now all the parts of the optical system are defined, a prototype can be created. This prototype has to be built up out of modular parts in order to make the system adaptable to different mirror distances. The prototype will be designed such that it can be used on a horizontal plane (such as a table) and to scan lifeless objects (such as wooden blocks). This simplifies the total system setup because there is no longer a need for a support of the human hand. In this way the prototype is still quite primitive, but the theoretical model as discussed in the previous chapters can be applied. The prototype will consist out of the following components (see Figure 9.1 in Section 9.1):

- Scanning system (projector and camera)
- Total of five mirrors:
  - Set of two mirrors at mirror position 1
  - Mirror at mirror position 2
  - Two mirrors at mirror position 3 and 4

#### 9.3.1 The scanning system

The scanning system is mounted on a red mounting rack (see Section 4.1) and is delivered by DAVID. This mounting rack is fastened on a tripod which stands on the ground; this construction makes it possible to define the height and the orientation of the mounting rack. The only properties that can be changed on the mounting rack are the distance between the scanner and the projector ( $V$ ) and the orientation of the camera relative to the projector ( $\lambda$ ) (see Chapter 4 and 5). The remainder of the scanning system is fully defined, therefore this scanning system is not treated further in detail.

### 9.3.2 The two mirrors at mirror position 1

In Section 9.2 the dimension of the mirrors are determined. These mirrors will be fastened in a metal slit, as illustrated in Figure 9.5 and 9.6.



**Figure 9.5** The metal slit with the two mirrors, the left one for the camera and the right one for the projector

The sizes of these two mirrors are equal to those calculated in Section 9.2, although a little adaption is done in such a way that these mirrors can be fastened correctly in the metal slit. The height of the metal slit is 33 mm and therefore the calculated heights are increased with 33 mm. The fastening of the mirrors is done by elastic parts which clamp the mirrors to the metal.



**Figure 9.6** Assembly of the mirrors

These elastic parts (see Figure 9.6) have been designed in Solidworks and printed with a 3D printer [S4,C4]. The elasticity of the clamping parts makes it possible to slide the mirrors in the metal slit smoothly to the desired distance. The advantage of this design is that by definition both mirrors are inclined parallel to each other and that the mirror distance ( $h_1$ ) can be varied by moving the metal slit on the table (or on another horizontal plane).

### 9.3.3 Mirror at mirror position 2

The mirror at position 2 is located behind the scanning system and therefore the mirror suspension needs to be installed on the ground (such as the tripod of the scanning system). This means that the mirror has to be positioned at a certain height to compensate the height difference that is present between the ground and the table plane. This is achieved by a 3D printed component which can be mounted on a tripod (which stands on the ground) [S5,C5] see Figure 9.7 and 9.8.



**Figure 9.7** The 3D printed component of which the screw clamps the mirror on to the edge.



**Figure 9.8** Component installed on the tripod

With the use of this component it is possible to rotate and move the tripod and mirror together as whole, while the mirror stays perpendicular to the ground, when adapting the mirror distance  $Z_T$ .

### 9.3.4 Mirrors at mirror position 3 and 4

The mirrors at position 3 and 4 have equal properties and therefore these mirrors can be designed identically. These mirrors have to be located perpendicular to the table and the angle between these two mirrors needs to be equal to  $90^\circ$ . This is achieved by using two external parts; one part is the table clamp which is originally used in the SaebomASS (see Figure 9.9) and the other part is the mounting track from DAVID that is used gain perpendicular calibration panels.

The mounting track ensures that the two mirrors are fastened to each other in the desired orientation ( $90^\circ$  angle difference). In this way it is possible to position these two mirrors together as whole when adapting the mirror distance  $Z_B$ .



Figure 9.9 Clamp with mirror

### 9.3.5 Overview of the complete prototype

The components that are present in the prototype have been discussed in the previous section. It should be noticed that the designs of all these components are based on parts that are produced within Hankamp. In Figure 9.10 the total prototype during a scanning process is shown.



Figure 9.10 Overview of the prototype during a scanning process; the numbers are explained in the main text

In Figure 9.10 the separate components discussed in Section 9.3 can be recognized:

1. The scanning system discussed in Section 9.3.1 (the non-visible camera is behind the mirror)
2. The critical mirror system discussed in Section 9.3.2
3. The mirror behind the scanning system on the tripod discussed in Section 9.3.3
4. The two mirrors from the bottom mirror system discussed in Section 9.3.4
5. The top side of the object that has to be scanned

These modular components are combined together according to the reduced coupling equation in Section 7.3.4 and the other design choices made in Chapter 7.

#### 9.4 Results of the prototype

With the prototype setup discussed in the previous section two scanning sessions of two different objects have been performed. The first object was the wooden rod that is also used in Section 7.3 and is shown in Figure 9.11 (and is also component 5 in Figure 9.10 in the previous section). The second object is a more complex wooden object, see Figure 9.13. The resulted images of these processes will be shown in this section.



**Figure 9.11** The simple wooden rod

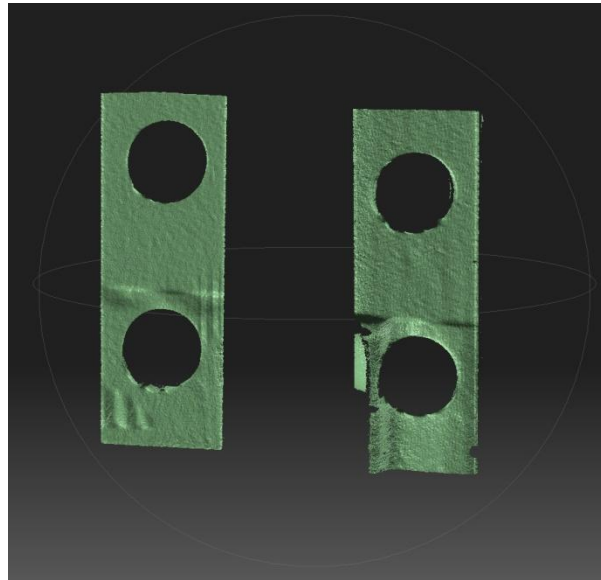


**Figure 9.12** The scanned images made with the prototype

Figure 9.12 shows the resulting image of the scanned wooden rod in Figure 9.11, on the left the front side is shown and on the right the back side [D1].



**Figure 9.13** The more complex beam

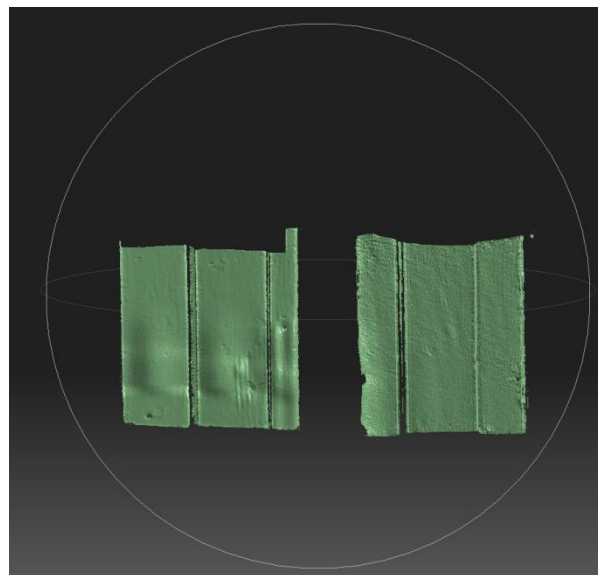


**Figure 9.14** The scanned image made with the prototype

Figure 9.14 shows the image of the scanned wooden beam presented in Figure 9.13, on the left the front side and on the right the back side [D2].

## 9.5 Discussion

In this section the results of the scanning processes described in the previous section are discussed.

The images of the scans in Section 9.4 are pretty good results, since they possess a big amount of detail and the sizes of the front and the back side are comparable. However, in Figure 9.12 part of the image of the back side is missing and the same is happened to the front side in Figure 9.14. This means that the camera beams are blocked on their way from the object.

Furthermore, the positions of the front and back side of the object are not exactly in line with each other, which is due to the primitive setup of the prototype. Position and orientation errors are easily made and the components are not fixated to the outside, which leads to inaccuracy in the results. Also there exists significant difference in the vertical position of the front and back side in Figure 9.12. This is caused by the fact that the mirrors are not exactly perpendicular to the ground and the table.

Especially the mirror behind the scanning system (component 3 in Figure 9.10 in Section 9.3.5) is not orientated well; which is caused by an inaccuracy in the tripod. This tripod automatically leans backward and therefore the effectivity of the total mirror system is disturbed. In case of the scanning process of the more complex wooden object, this was corrected by placing a piece of cardboard under one of the feet of the tripod. In Figure 9.14 it can be seen that this is an effective connection and that the vertical position difference has become nearly negligible.

Likewise the fact that the modular components are not fixated is troublesome, since during the installation of a component another component can easily be touched and shifted. Of course this will lead to errors in the results.

## 9.6 Conclusions

The first topic that has to be further investigated is the camera range, since the images are not fully visible. Besides that, not the same part of the images in Figure 9.12 and 9.14 are missing. The blockages of the camera range have to be located and eliminated. Possible blockages could be one or more trespassing mirrors or supporting parts of the scanning system.

A second topic is that assembling errors have significant influence on the results. This prototype is too primitive for gaining reliable results that can be coupled together using the algorithm that is discussed in Chapter 8. The inaccuracies present in the current setup prevent a good coupling process. This means that a setup is needed where the modular parts are fixated precisely in such a way that extern factors, such as vibrations, have no consequences for the performance of the total system.

The even more important advantage of a fixated system is that when a component is installed correctly this component holds its orientation and stays on exact the same position. This means that when the system is fully calibrated, the configuration of the system is exactly known and the coupling can be performed each time under the same boundary conditions (rotation will be performed in the same coordinate system).

As an overall conclusion, the working principles have already been demonstrated and confirmed. This means that this prototype can serve as basis for further research and investigation.

## 10 Manual for using the total system

This chapter consists of a manual with which one is able to work with the prototype discussed in the previous chapter. This manual describes the steps that are required to make similar scans as shown in the figures in Section 9.4. In this manual it is assumed that the reader is known with the working principles of the DAVID scanning system and has read the relevant associated documents [2,5]. For this manual a special Matlab script is created that generates the needed values for the setup of the prototype [M19].

### 10.1 Preparation

Firstly the generic conditions must become fulfilled. The degree of ambient light in the system has to be controlled and therefore a room sealed from ambient light is desirable. In this room a stable horizontal table must be present. Such that this table can serve as a mounting plane for the setup.

Secondly, the characteristics of the scanning system have to be adapted to a scanning distance of 650 mm (E). This means that the focus, the amount of light and the distance between the camera and the projector (V) are adapted to this scanning distance. Using the equation for the distance V of Section 4.5 yields:

$$V = 0.35714 \times 650 - 1.42857 \approx 231 \text{ mm}$$

This means that the red mounting rack distance between the lenses of the projector and the camera is approximately around 231 mm. The values of the amount of light and the focus have to be adjusted using an object at a scanning distance of 650 mm, which has similar geometrical and external properties as the object that needs to be scanned (or the scanned object itself can be used).

Subsequently, orientate the camera such that the whole object becomes visible in the software and that preferably the coordinate system of the camera and the projector do overlap. This overlapping makes the combining process as easily as possible (in order to use the combining method described in Chapter 8 one has to know the characteristics of the coordinate system with respect to the scanned object). When the camera is orientated well the angle  $\lambda$  is around  $73^\circ$  (see Section 5.5).

Finally, the screws of the projector and the camera have to be fastened firmly and the properties of the camera and the projector have to be unmodified in order to ensure that the characteristics of the scanning system remain the same. The system is now ready for calibration, so calibrate the system. Once calibrated, you may move, rotate and tilt the scanner as a whole, and you can close and restart the DAVID software, without losing the calibration settings. Therefore it is important that this preparation is done correctly, so that the same scanning system can be used multiple times.

The scanning system is now ready to become positioned in the total system. Take care that during the preparation no mirrors are used at all. Ensure that the properties of the scanning system do not change during the installation stage and the scanning process. This enables the use of the scanning system multiple times in different (mirror) setups.

### 10.2 Installation of the components in the setup

This section contains the installation steps of the different components that are needed to complete the total setup properly. The instructions will be given using the components illustrated in Figure 9.10 of Section 9.3.5. This can only be executed when the scanning system is calibrated correctly, as described in the previous section.

#### 10.2.1 Top mirrors and scanning system

The first step is to determine the position of the two mirrors, this is done by choosing the two mirror distances  $h_1$  and  $Z_T$ . The boundary conditions for these distances are (distances are in mm):

$$0 \leq h_1 \leq 125.8623 \quad (\text{see Section 9.2.2})$$

$$(A + h_1) \ll Z_T < (\cos(\Omega) E - h_1)/2 \quad (\text{see Figure 10.1 on the next page})$$

These two intervals are based on the facts that the second mirror needs to be installed behind the projector and that the projection area is behind the first mirror (the scanning distance to the first mirror is maximal 650 mm, as illustrated in Figure 10.1).

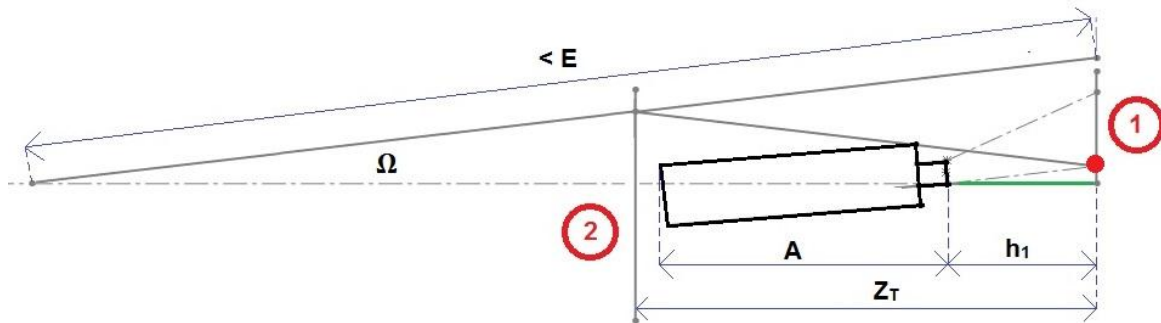


**Figure 10.1** The scanning system inclined under a vertical angle  $\Omega$

The chosen values of  $h_1$  and  $Z_T$  have to be supplied to the Matlab script [M19]; this script calculates the minimum tilt angle and checks if the boundary conditions are fulfilled. If you receive the message 'Good values' then the parameters of the top system are installed correctly and the next step can be performed. Otherwise you have to decrease the ratio  $h_1/Z_T$  and you have to repeat this step.

The next step is to install the scanning system such that the lens of the projector is set against the edge of the table (green line in Figure 10.1). This can be done by varying the tripod in height and rotating the mounting rack by turning the big knob. This has to be done such that the lowest ray of the projection pattern arrives just above the top edge of the metal slit of the casing of the first mirrors, as illustrated in Figure 9.5 in Section 9.3.2; this is also shown in Figure 10.1 with the red dot.

In this way the mirrors are optimally used and the beams to the bottom mirror system can pass over the metal slit. During this action ensure that the distance between the edge of the table and the front side of the first mirror is equal to the chosen value of  $h_1$  and that the metal slit is orientated parallel with the projector lens, as is shown in Figure 10.2. The vertical tilt angle  $\Omega$  is approached by this action.

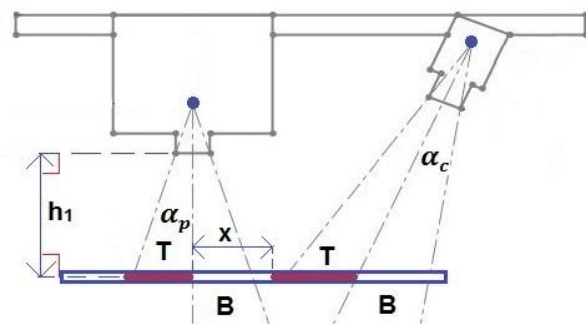


**Figure 10.2** Installing the mirrors at position 1

The following step is to adjust the open space in the metal slit between the two mirrors (distance  $x$  in Figure 10.2); this can be done by shifting the flexible parts. This has to be done such that the left side of the projector mirror is exactly in the centre of the projection pattern and at the same time the left side of the camera mirror is coinciding with the vertical axis of the camera coordinate system. In this way the range of the scanning system is splitted into two equal halves, see Figure 10.3. During this the orientation and the position of the metal slit should not be modified.



**Figure 10.3** Placement of the camera mirror

The final step in this section is the placement of the mirror at position 2. The position of it must be such that it reflects all the beams coming from the mirrors at position 1. The orientation of the mirror is predefined because it is required that the mirror is parallel with the mirrors at position 1.

The value  $Z_T$  is already chosen in the begin of this section and therefore the mirror can only move in a 2D plane. This can be achieved by adapting the height of the mirror tripod and moving the tripod in a direction parallel with the mirrors at position 1. The obtained setup so far is shown in Figure 10.4.

When this illustrated top mirror setup is obtained, the next step can be performed: the installing of the bottom mirrors (next section).

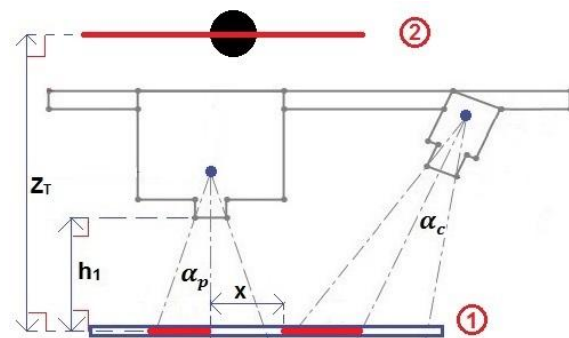


Figure 10.4 Installation of the mirror at position 2

**10.2.2 Bottom mirrors**

The installation of the bottom mirrors is a relatively easy step. The only parameter needed to install the bottom mirrors is the mirror distance  $Z_B$ . This distance is calculated using the reduced coupling equation (see Section 7.3.4) in the Matlab script [M19].

This value of  $Z_B$  has to be used to install the two mirrors, which are inclined under a angle of  $90^\circ$  relative to each other by the mounting track of DAVID. The important part of this installation is that the inclination point of the two mirrors (3 and 4) has to be in line with the bisector of the projector (so this point is aligned vertically with the projector centre as illustrated in Figure 10.5).

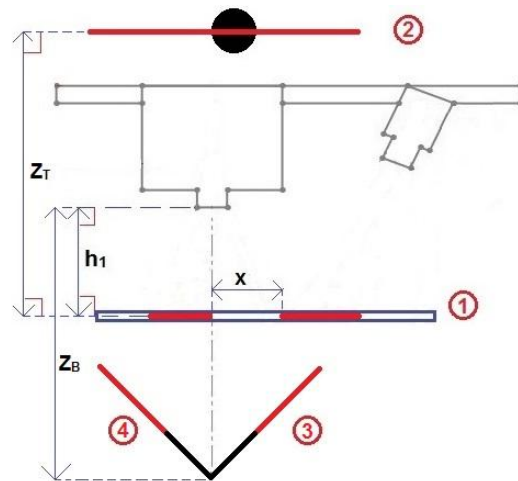


Figure 10.5 Installation of the mirrors at the bottom

**10.2.3 Placement of the desired scan object**

Now the total setup is created, the object that needs to be scanned can become placed. This has to be done such that the optical lengths of the bottom and top mirror system to the object are equal. This position can be calculated using the same principles as in Chapter 7.

Furthermore, the two scanned images have to be combinable and therefore the back side of the object (seen from the projector) has to be on the focus plane as is discussed in Section 8.5. Therefore the generated value of  $F$  by the Matlab script [M19] has to be implemented in the total setup as shown in Figure 10.6. It is also important that the edges of the object (SO in Figure 10.6) are on the left side of the bisector of the projector, otherwise the setup does not work correctly and only a part of the object will be scanned. The height and the horizontal position of the object have to be varied such that the whole object is visible by the projector (at the position  $F$ ). This height is dependent of the tilt angle and therefore a modular support is needed.

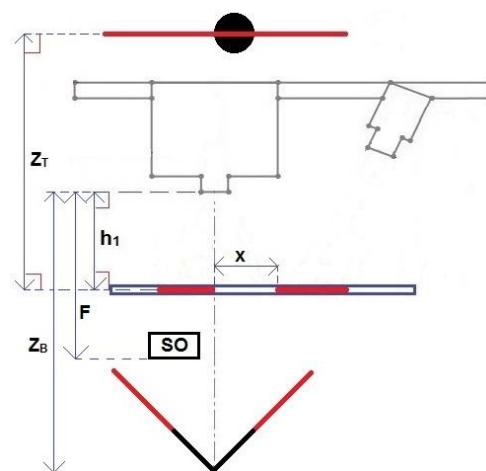


Figure 10.6 Placement of the scan object in the total setup

### 10.3 Control and performance of the scan

Check the view in the DAVID software and verify if you can see both sides of the object at a similar orientation and position. If this is not the case, you have to check if you did not have made any assembling errors. When you detect any error try to adapt it without modifying other properties of the setup. If this is not possible you have to repeat all steps described in Section 10.2.

When the right images are obtained in the DAVID software you are ready to make a scan. During the scan ensure that the same conditions are obtained as during the calibration process. After the scan is made, you have to remove the noise and other undesired features of the image and export the scan in an OBJ file format [2,5].

When you have adapted the scanning process such that you meet the initial requirements of the combining process as discussed in Section 8.5, the generated OBJ file can be loaded into the available combining algorithm [M16].

## 11 Conclusion and recommendations

The goal of this report was to provide an answer to the formulated research question:

*“Is it possible to create an automatic process which makes a complete 3D scan of the hand, using mirrors to obtain two simultaneous scans and a mathematical software package to combine these individual scans, to gain a custom fitted hand orthosis which can be printed by a 3D printer?”*

The answer to this question is yes, it is possible, but only if many requirements are met. In this report the problem was analyzed using a self-made mathematical model. Based on this solution a primitive setup was created which is able to scan two sides of the hand simultaneously and is in principle also able to combine these two images of the hand into a full 3D image of the hand. Also this report contains a manual describing a step-by-step procedure to enable proper working with this prototype.

However, this prototype is too primitive to perform the entire procedure and therefore the first step that must be taken is the further improvement of this prototype. This can be realized by creating a setup which is built up out of components which can be accurately fastened to a frame. But at the same time these components have to be adjustable for different scanning setups. With such an improved setup one is able to incorporate the influence of mirror thickness and one is able to improve the mathematical model and the coupling between the 2D and 3D models. Using this knowledge can ensure that the combining algorithm fits better to the scanning process such that the entire procedure can be further improved.

When this is successfully done and a satisfying 3D image can be obtained by the combination of the improved setup and the software, the setup (and the software) can become extended with more mirrors to scan more sides of the object. This can be realized by using mirrors which split the beams of the scanning system in more parts which are eventually reflected back to the object. This results in a smoother 3D image of the object.

The final step is to adapt this advanced system such that it becomes able to scan human hands. In order to enable this, a support for the hand has to be realized which does not interrupt the scanning process (for example a fully transparent glass plate). This total system has to be protected from dust and other disturbances such that the mirror systems keep working properly and the properties of the system remain optimally, such that this system can be used in rehabilitation. In this way a perfect custom fitted hand orthosis can be made for patients.

## 12 References

- [1] **Website Hankamp Rehab**  
<http://www.hankamprehab.nl/>
- [2] **Bachelor-Thesis Marcel Heinrich 2014**  
BachThesis\_Marcel Heinrich\_s1224514.pdf
- [3] **Report Internship Johannes van Wijngaarden**  
Stageverslag Johannes van Wijngaarden.pdf
- [4] **Website DAVID**  
<http://www.david-3d.com>
- [5] **Manual DAVID SLS-1**  
GSG\_EN\_3.9\_2013-10-02
- [6] **Website Ultimaker**  
<https://www.ultimaker.com/>
- [7] **Systematische Natuurkunde**  
Nijgh Versluys  
ISBN 978 90 425 3637 1
- [8] **Website DINED**  
<http://dined.io.tudelft.nl/dined/nl>

## 13 Generated software

### Matlab Scripts

- [M01] Mathematical\_Properties\_Projector.m
- [M02] Mathematical\_Properties\_Camera.m
- [M03] Camera\_Projector\_Distance.m
- [M04] Position\_Reflection.m
- [M05] Bottom\_Mirror\_System.m
- [M06] Top\_Mirror\_System.m
- [M07] Test\_Bottom\_Distances.m
- [M08] Test\_Bottom\_Angles.m
- [M09] Test\_Top\_Distances.m
- [M10] Test\_Top\_Angles.m
- [M11] Coupling\_Equation.m
- [M12] Rotation\_Properties.m
- [M13] Performing\_Rotation.m
- [M14] Rotation\_Focus\_Top.m
- [M15] Rotation\_Focus\_Bottom.m
- [M16] Combining\_Algorithm.m
- [M17] H1max\_and\_H1min.m
- [M18] Vertical\_Tilt\_Angle.m
- [M19] Manual.m
- [M20] Elimination\_of\_Z1T.m

### SolidWorks Files

- [S01] Mirror\_Setup.sldprt
- [S02] Design\_Setup.sldprt
- [S03] Influence\_Vertical\_Angle.sldprt
- [S04] Clamping\_Mirror\_Position\_1.sldprt
- [S05] Clamping\_Mirror\_Position\_2.sldprt

### Cura Files

- [C04] Clamping\_Mirror\_Position\_1.stl
- [C05] Clamping\_Mirror\_Position\_2.stl

### DAVID Files

- [D01] Wooden\_Rod.obj
- [D02] Complex\_Beam.obj

## **A. Appendices**

- I. Appendix A1 Relationships of the mirrors**
- II. Appendix A2 Position of the imaginary point sources**
- III. Appendix A3 Independency of the top mirror parameter**
- IV. Appendix A4 Reducing the equations for the imaginary point sources**
- V. Appendix A5 Calculation of the minimum and maximum first mirror distance**
- VI. Appendix A6 Calculation of the minimum vertical tilt angle**

**I. Appendix A1 Relationships of the mirrors**

One or two mirrors

For the analysis of these situations Figure A1.1 is used. With the use of geometry the following comparisons for the reflection angles can be obtained:

$$A_1 = \alpha \quad (\text{because of Z-angles})$$

$$A_2 = \theta \quad (\text{because of F-angles})$$

$$\beta = A_1 + A_2 = \theta + \alpha$$

$$\gamma + \theta + \varphi + \beta = 180^\circ \quad (\text{sum angle of triangle})$$

$$\gamma = C_1 = 180^\circ - \theta - \varphi - \beta = 180^\circ - 2\theta - \alpha - \varphi$$

Same angle of incidence with one mirror if:

$$A_{13} = \alpha$$

$$180^\circ - \beta - \theta = \alpha$$

$$180^\circ - 2\theta - \alpha = \alpha$$

$$\theta = 90^\circ - \alpha$$

Same angle of incidence with two mirror if:

$$C_2 = \alpha$$

$$90^\circ - (90^\circ - \varphi) - \gamma = \alpha$$

$$\varphi - (180^\circ - 2\theta - \alpha - \varphi) = \alpha$$

$$\varphi + \theta = 90^\circ$$

Three or four mirrors

For the analysis of these situations Figure A1.2 is used. With the use of geometry the following comparisons for the reflection angles can be obtained:

$$\beta = \theta + \alpha \quad (\text{see above})$$

$$\gamma = -180^\circ - (180^\circ - 2\beta) - (-\varphi + \alpha)$$

$$\gamma = \varphi + 2\theta + \alpha$$

$$\delta = \psi + \varphi + \gamma$$

$$\delta = \psi + \varphi + (\varphi + 2\theta + \alpha)$$

$$\delta = \psi + 2\varphi + 2\theta + \alpha$$

$$\delta + \psi + \omega + \varepsilon = 180^\circ \quad (\text{sum angle of triangle})$$

$$\varepsilon = E_1 = 180^\circ - \psi - \omega - \delta$$

$$\varepsilon = 180^\circ - \psi - \omega - (\psi + 2\varphi + 2\theta + \alpha)$$

$$\varepsilon = 180^\circ - 2\psi - 2\varphi - \omega - 2\theta - \alpha$$

Same angle of incidence

- with three mirrors if:

$$C_{13} = \alpha$$

$$180^\circ - \delta - \psi = \alpha$$

$$180^\circ - 2\psi - 2\varphi - 2\theta - \alpha = \alpha$$

$$\psi + \theta + \varphi = 90^\circ - \alpha$$

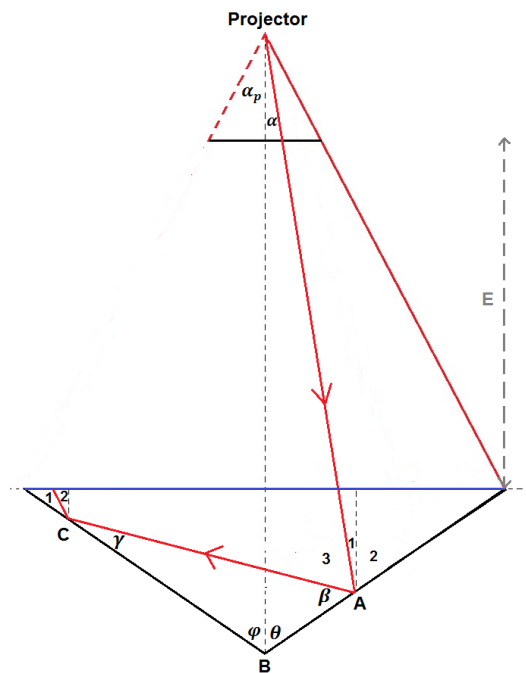


**Figure A1.1** The mirror setup with one or two mirrors, the blue line represent the surface of projection.

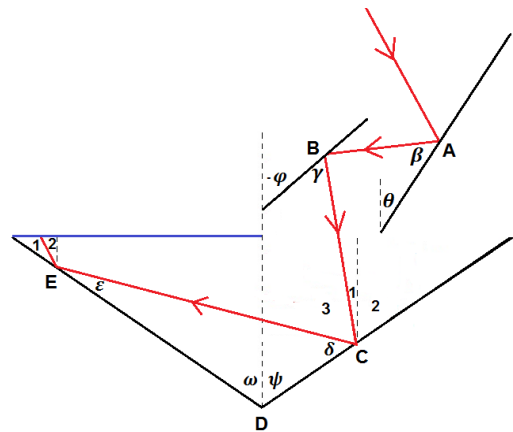


**Figure A1.2** The mirror setup with three or four mirrors, the blue line represent the surface of projection.

- with four mirrors if:

$$E_2 = \alpha$$

$$90^\circ - (90^\circ - \omega) - \varepsilon = \alpha$$

$$\omega - (180^\circ - 2\psi - 2\varphi - \omega - 2\theta - \alpha) = \alpha$$

$$\psi + \omega + \theta + \varphi = 90^\circ$$

II. Appendix A2 Position of the imaginary point sources

In Figure A2.1 a point source (p) and his imaginary point sources ( $p_{i1}$  and  $p_{i2}$ ) are shown. These points are created by the two mirrors shown in red. The first mirror is responsible for  $p_{i1}$  and the second mirror is responsible for  $p_{i2}$ . The two mirrors are fully defined by choosing the angle of inclining ( $\alpha$  and  $\beta$ ) and the height of this inclining point ( $Z_1$  and  $Z_2$ ). When the position of p is choosing equally to the point source of the projector or the camera, it is possible to calculate where its imaginary point source is located ( $p_{i2}$ ).

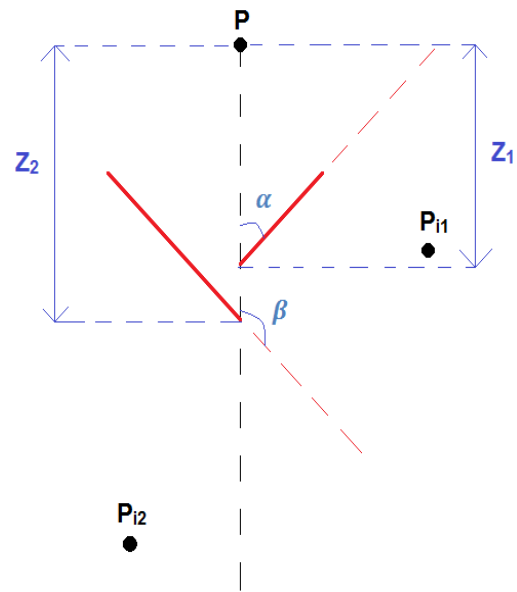


Figure A2.1 A mirror setup with two (red) mirrors and two created imaginary points

The following equations can be obtained for the coordinates of the first mirror ( $x_{m1}$  and  $y_{m1}$ ):

$$y_{m1} = ax_{m1} + b$$

$$b = Z_1$$

$$a = \frac{1}{\tan(\alpha)}$$

$$y_{m1} = \frac{x_{m1}}{\tan(\alpha)} - Z_1$$

With this known, it is possible to calculate the distance of point p to the mirror ( $d_{1p}$ ). This is done using the coordinates of point p ( $x_p$  and  $y_p$ ) and a point on the first mirror ( $x_{m1}$  and  $y_{m1}$ ):

$$d_{1p} = \sqrt{(x_{m1} - x_p)^2 + (y_{m1} - y_p)^2} = \sqrt{(x_{m1} - x_p)^2 + \left(\frac{x_{m1}}{\tan(\alpha)} - Z_1 - y_p\right)^2}$$

$$d_{1p} = \sqrt{x_{m1}^2 + x_p^2 - 2x_px_{m1} + \frac{x_{m1}^2}{\tan^2(\alpha)} - (Z_1 + y_p)^2 - 2\frac{x_{m1}(Z_1 + y_p)}{\tan(\alpha)}}$$

When it is known for which point on the mirror this distance is minimized, the location of the first imaginary point can be obtained. Furthermore, when  $d_{1p}^2$  is minimized, also  $d_{1p}$  is as small as possible:

$$d_{1p}^2 = x_{m1}^2 + x_p^2 - 2x_px_{m1} + \frac{x_{m1}^2}{\tan^2(\alpha)} - (Z_1 + y_p)^2 - 2\frac{x_{m1}(Z_1 + y_p)}{\tan(\alpha)}$$

$$\frac{d_{1p}^2}{x_{m1}} = 2x_{m1} - 2x_p + 2\frac{x_{m1}}{\tan^2(\alpha)} - 2\frac{(Z_1 + y_p)}{\tan(\alpha)}$$

When the centre of the coordinate system is chosen smartly, so when the centre coincides with the point p, this leads to that  $x_p = y_p = 0$ . The obtained equation reduces to:

$$\frac{d_{1p}^2}{x_{m1}} = 2x_{m1} + 2\frac{x_{m1}}{\tan^2(\alpha)} - 2\frac{Z_1}{\tan(\alpha)}$$

The point on the mirror where the distance is minimized can now be calculated:

$$\frac{d_{1p}^2}{x_{m1}} = 0 = 2x_{m1} + 2\frac{x_{m1}}{\tan^2(\alpha)} - 2\frac{Z_1}{\tan(\alpha)}$$

$$\frac{2x_{m1} \tan^2(\alpha)}{\tan^2(\alpha)} + 2 \frac{x_{m1}}{\tan^2(\alpha)} - 2 \frac{Z_1}{\tan(\alpha)} = 0$$

$$\frac{x_{m1} \tan^2(\alpha) + x_{m1}}{\tan^2(\alpha)} = x_{m1} \frac{(\tan^2(\alpha) + 1)}{\tan^2(\alpha)} = \frac{Z_1}{\tan(\alpha)}$$

$$x_{m1} = \frac{Z_1 \tan^2(\alpha)}{\tan(\alpha) (\tan^2(\alpha) + 1)} = \frac{Z_1 \tan(\alpha)}{(\tan^2(\alpha) + 1)}$$

With this value the y-coordinate of the inclining point can be calculated:

$$y_{m1} = \frac{x_{m1}}{\tan(\alpha)} - Z_1 = \frac{Z_1}{(\tan^2(\alpha) + 1)} - Z_1 = \frac{Z_1(1 - (\tan^2(\alpha) + 1))}{(\tan^2(\alpha) + 1)} = -\frac{Z_1 \tan^2(\alpha)}{(\tan^2(\alpha) + 1)}$$

With the inclining coordinates known, it is possible to determine the first imaginary point ( $p_{i1}$ ):

$$x_{p_{i1}} = x_{m1} + (x_{m1} - x_p) = 2x_{m1} = 2 \frac{Z_1 \tan(\alpha)}{(\tan^2(\alpha) + 1)}$$

$$y_{p_{i1}} = y_{m1} + (y_{m1} - y_p) = 2y_{m1} = -2 \frac{Z_1 \tan^2(\alpha)}{(\tan^2(\alpha) + 1)}$$

The second imaginary point can be determined with the same principle as used above and the obtained coordinates for the imaginary point (see Figure A2.1 again):

$$y_{m2} = \frac{x_{m2}}{\tan(\beta)} - Z_2$$

$$d_{2p} = \sqrt{(x_{m2} - x_{p_{i1}})^2 + (y_{m2} - y_{p_{i1}})^2} = \sqrt{(x_{m2} - x_{p_{i1}})^2 + \left(\frac{x_{m2}}{\tan(\beta)} - Z_2 - y_{p_{i1}}\right)^2}$$

This results in (for the intermediate steps, see the operation above):

$$\frac{d_{2p}^2}{x_{m2}} = 2x_{m2} - 2x_{p_{i1}} + 2 \frac{x_{m2}}{\tan^2(\beta)} - 2 \frac{(Z_2 + y_{p_{i1}})}{\tan(\beta)} = 0$$

The point on the mirror where the distance is minimized can now be calculated:

$$2x_{m2} + 2 \frac{x_{m2}}{\tan^2(\beta)} = 2x_{p_{i1}} + 2 \frac{(Z_2 + y_{p_{i1}})}{\tan(\beta)}$$

$$\frac{x_{m2} \tan^2(\beta)}{\tan^2(\beta)} + \frac{x_{m2}}{\tan^2(\beta)} = \frac{x_{m2} (\tan^2(\beta) + 1)}{\tan^2(\beta)} = x_{p_{i1}} + \frac{(Z_2 + y_{p_{i1}})}{\tan(\beta)}$$

$$x_{m2} = \left(x_{p_{i1}} + \frac{(Z_2 + y_{p_{i1}})}{\tan(\beta)}\right) \left(\frac{\tan^2(\beta)}{(\tan^2(\beta) + 1)}\right) = \frac{x_{p_{i1}} \tan^2(\beta)}{(\tan^2(\beta) + 1)} + \frac{(Z_2 + y_{p_{i1}}) \tan(\beta)}{(\tan^2(\beta) + 1)}$$

$$x_{m2} = \frac{x_{p_{i1}} \tan^2(\beta) + (Z_2 + y_{p_{i1}}) \tan(\beta)}{(\tan^2(\beta) + 1)}$$

With this value the y-coordinate of the inclining point can be calculated:

$$y_{m2} = \frac{x_{m2}}{\tan(\beta)} - Z_2 = \frac{x_{p_{i1}} \tan(\beta) + Z_2 + y_{p_{i1}}}{(\tan^2(\beta) + 1)} - Z_2 = \frac{x_{p_{i1}} \tan(\beta) + Z_2 + y_{p_{i1}}}{(\tan^2(\beta) + 1)} - \frac{Z_2 (\tan^2(\beta) + 1)}{(\tan^2(\beta) + 1)}$$

$$y_{m2} = \frac{x_{pi1} \tan(\beta) + y_{pi1} - Z_2 \tan^2(\beta)}{(\tan^2(\beta) + 1)}$$

With these inclining coordinates known, it is possible to determine the coordinates of the second imaginary point ( $p_{i2}$ ):

$$x_{pi2} = x_{m2} + (x_{m2} - x_{pi1}) = 2 \frac{x_{pi1} \tan^2(\beta) + (Z_2 + y_{pi1}) \tan(\beta)}{(\tan^2(\beta) + 1)} - 2 \frac{Z_1 \tan(\alpha)}{(\tan^2(\alpha) + 1)}$$

$$y_{pi2} = y_{m2} + (y_{m2} - y_{pi1}) = 2 \frac{x_{pi1} \tan(\beta) + y_{pi1} - Z_2 \tan^2(\beta)}{(\tan^2(\beta) + 1)} + 2 \frac{Z_1 \tan^2(\alpha)}{(\tan^2(\alpha) + 1)}$$

With the position of the second imaginary point known, it is possible to determine the position of the imaginary point sources above the hand and the imaginary point sources below the hand. To make this possible, first the new variables  $Z_{1B}$ ,  $Z_{2B}$ ,  $Z_{1T}$  and  $Z_{2T}$  must be introduced. Together with the already introduced inclining angles  $\theta$ ,  $\varphi$ ,  $\psi$  and  $\omega$  it is possible to make the obtained equations for the coordinates of  $p_{i2}$  suitable for the two kinds of mirror systems (top and bottom). The variables will be presented respectively in Figure A2.2 and A2.3 below.

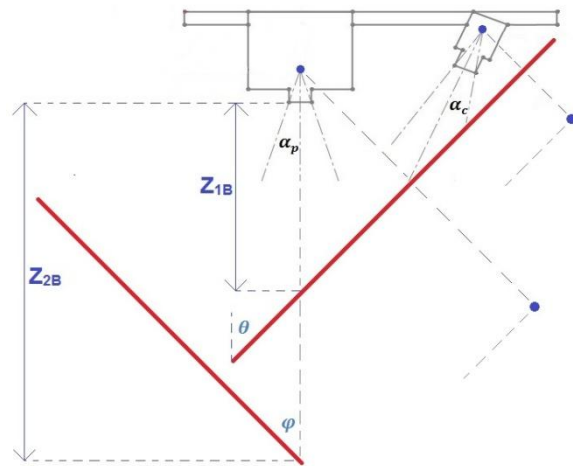
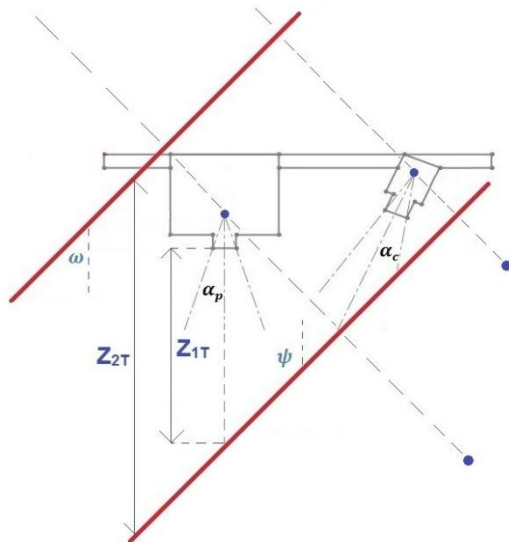


Figure A2.2 Variables of the top mirror system

Figure A2.3 Variables of the bottom mirror system

With the use of these figures it is possible to express the parameters in the obtained equations for the coordinates of  $p_{i2}$  in the variables for the top and the bottom systems. The substitution values for the projector are summed up in Table A2.1 below.

Table A2.1 Substitution values of the projector for the top and the bottom mirror system

Parameter	above the hand (Top)	below the hand (Bottom)
$Z_1$	$Z_{1T} + (90 - SD_p)$	$Z_{1B} + (90 - SD_p)$
$Z_2$	$Z_{1T} + (90 - SD_p) - Z_{2T}$	$Z_{2B} + (90 - SD_p)$
$\alpha$	$180^\circ - \psi$	$\theta$
$\beta$	$\omega$	$180^\circ - \varphi$

The coordinates of the imaginary point sources can be determined with substitution of the values listed in table x. The results of this substitution are listed on the next page.

Coordinates of the imaginary projector point source of the bottom mirror system ( $x_{PSB}$  and  $y_{PSB}$ ):

$$x_{PSB} = 2 \frac{x_{pi1B} \tan^2(180^\circ - \varphi) + (Z_{2B} + (90 - SD_p) + y_{pi1B}) \tan(180^\circ - \varphi)}{(\tan^2(180^\circ - \varphi) + 1)} - 2 \frac{(Z_{1B} + (90 - SD_p)) \tan(\theta)}{(\tan^2(\theta) + 1)}$$

$$y_{PSB} = 2 \frac{x_{pi1B} \tan(180^\circ - \varphi) + y_{pi1B} - (Z_{2B} + (90 - SD_p)) \tan^2(180^\circ - \varphi)}{(\tan^2(180^\circ - \varphi) + 1)} + 2 \frac{(Z_{1B} + (90 - SD_p)) \tan^2(\theta)}{(\tan^2(\theta) + 1)}$$

With:

$$x_{pi1B} = 2 \frac{(Z_{1B} + (90 - SD_p)) \tan(\theta)}{(\tan^2(\theta) + 1)}$$

$$y_{pi1B} = -2 \frac{(Z_{1B} + (90 - SD_p)) \tan^2(\theta)}{(\tan^2(\theta) + 1)}$$

Coordinates of the imaginary projector point source of the top mirror system ( $x_{PST}$  and  $y_{PST}$ ):

$$x_{PST} = 2 \frac{x_{pi1T} \tan^2(\omega) + (Z_{1T} + (90 - SD_p) - Z_{2T} + y_{pi1T}) \tan(\omega)}{(\tan^2(\omega) + 1)} - 2 \frac{(Z_{1T} + (90 - SD_p)) \tan(180^\circ - \psi)}{(\tan^2(180^\circ - \psi) + 1)}$$

$$y_{PST} = 2 \frac{x_{pi1T} \tan(\omega) + y_{pi1T} - (Z_{1T} + (90 - SD_p) - Z_{2T}) \tan^2(\omega)}{(\tan^2(\omega) + 1)} + 2 \frac{(Z_{1T} + (90 - SD_p)) \tan^2(180^\circ - \psi)}{(\tan^2(180^\circ - \psi) + 1)}$$

With:

$$x_{pi1T} = 2 \frac{(Z_{1T} + (90 - SD_p)) \tan(180^\circ - \psi)}{(\tan^2(180^\circ - \psi) + 1)}$$

$$y_{pi1T} = -2 \frac{(Z_{1T} + (90 - SD_p)) \tan^2(180^\circ - \psi)}{(\tan^2(180^\circ - \psi) + 1)}$$

The same principles can be applied to the point source of the camera, this is not elaborated here. However, this process can be viewed in Matlab [M5,M6]. The underlying idea of this appendix is to show that this method is applicable to every point source.

Furthermore a Solidworks Model is created that give a visualization of the top and bottom mirror system [S1]. In this model two items are created named TOP and BOTTOM, which show respectively the top and bottom mirror system. Overviews of these items are shown on the next page in Figure A2.4 and A2.5.

The values in SolidWorks correspond with the values in Matlab, this means that the Solidworks gives a visualization of the calculations executed in Matlab. Same input parameters result in the same coordinates for the imaginary point sources.

*Note: When performing a simulation in Solidworks, the rebuild button (traffic light sign) have to be selected to ensure that the simulation is executed properly.*

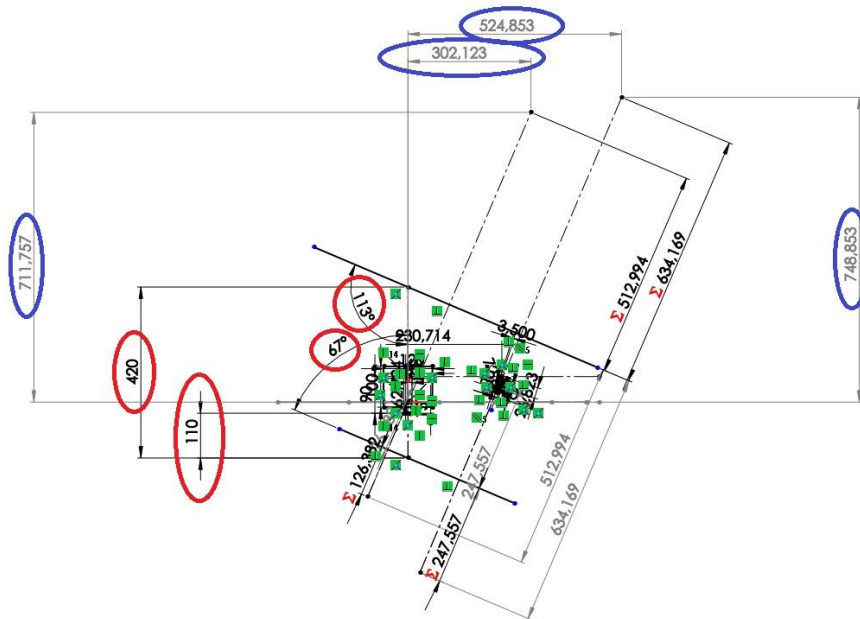


**Figure A2.4** Overview of the top mirror system, the input parameters are encircled red and the coordinates of the imaginary point sources are encircled blue (dimensions in mm).

Figure A2.4 shows the top mirror system for the following parameters (red):  $Z_{1T} = 110 \text{ mm}$ ,  $Z_{2T} = 420 \text{ mm}$ ,  $\psi = 67^\circ$  and  $\omega = 113^\circ$ . This gives the following coordinates (blue in the figure): Imaginary projector point source: (302,1 ; 711,8) and Imaginary camera point source: (524,9 ; 748,9)

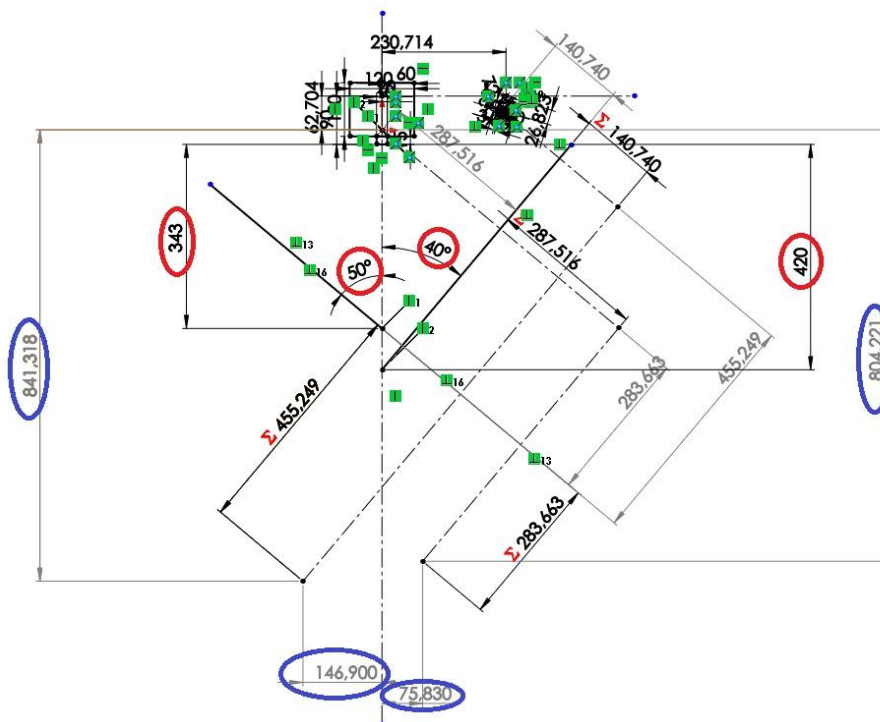


**Figure A2.5** Overview of the bottom mirror system, the input parameters are encircled red and the coordinates of the imaginary point sources are encircled blue (dimensions in mm).

Figure A2.4 shows the top mirror system for the following parameters (red):  $Z_{1B} = 420 \text{ mm}$ ,  $Z_{2T} = 343 \text{ mm}$ ,  $\psi = 40^\circ$  and  $\omega = 50^\circ$ . This gives the following coordinates (blue in the figure): Imaginary projector point source: (75,8 ; -804,2) and Imaginary camera point source: (-146,9 ; -841,3)

### III. Appendix A3 Independency of the top mirror parameter

In Section 7.3.2 there is stated that the obtained equations for  $x_{PST}$  and  $y_{PST}$  (see Appendix II) have to be independent of  $Z_{1T}$ . In this Appendix this statement will be proven analytically.

The x-coordinate of the imaginary projector point source ( $x_{PST}$ ):

First there is looked at the terms that consist of  $Z_{1T}$  in the equations of  $x_{PST}$  and  $y_{PST}$ . Let start with the equation of  $x_{PST}$ , terms containing any form of  $Z_{1T}$  are made bold:

$$x_{PST} = 2 \frac{x_{pi1T} \tan^2(\omega) + (\mathbf{Z}_{1T} + (90 - SD_p) - Z_{2T} + y_{pi1T}) \tan(\omega)}{(\tan^2(\omega) + 1)} - 2 \frac{(\mathbf{Z}_{1T} + (90 - SD_p)) \tan(180^\circ - \psi)}{(\tan^2(180^\circ - \psi) + 1)}$$

The independency must result in the following equation:

$$2 \frac{x_{pi1T} \tan^2(\omega) + (\mathbf{Z}_{1T} + (90 - SD_p) + y_{pi1T}) \tan(\omega)}{(\tan^2(\omega) + 1)} - 2 \frac{(\mathbf{Z}_{1T} + (90 - SD_p)) \tan(180^\circ - \psi)}{(\tan^2(180^\circ - \psi) + 1)} = 0$$

This equation can be simplified when  $Z_{1T} + (90 - SD_p)$  is taken equal to A:

$$2 \frac{A \tan(180^\circ - \psi)}{(\tan^2(180^\circ - \psi) + 1)} \tan^2(\omega) + A \tan(\omega) - 2 \frac{A \tan^2(180^\circ - \psi)}{(\tan^2(180^\circ - \psi) + 1)} \tan(\omega) - \frac{A \tan(180^\circ - \psi)}{(\tan^2(180^\circ - \psi) + 1)} = 0$$

$$\frac{2A \tan(180^\circ - \psi) \tan^2(\omega) + A \tan(\omega) (\tan^2(180^\circ - \psi) + 1) - 2A \tan^2(180^\circ - \psi) \tan(\omega)}{(\tan^2(\omega) + 1) (\tan^2(180^\circ - \psi) + 1)} - \frac{A \tan(180^\circ - \psi) (\tan^2(\omega) + 1)}{(\tan^2(\omega) + 1) (\tan^2(180^\circ - \psi) + 1)} = 0$$

$$2A \tan(180^\circ - \psi) \tan^2(\omega) + A \tan(\omega) (\tan^2(180^\circ - \psi) + 1) - 2A \tan^2(180^\circ - \psi) \tan(\omega) - A \tan(180^\circ - \psi) (\tan^2(\omega) + 1) = 0$$

Dividing by A results in the following equation:

$$2 \tan(180^\circ - \psi) \tan^2(\omega) + \tan(\omega) (\tan^2(180^\circ - \psi) + 1) - 2 \tan^2(180^\circ - \psi) \tan(\omega) - \tan(180^\circ - \psi) (\tan^2(\omega) + 1) = 0$$

$$\tan(180^\circ - \psi) \tan^2(\omega) + \tan(\omega) - \tan^2(180^\circ - \psi) \tan(\omega) - \tan(180^\circ - \psi) = 0$$

This equation is analyzed in Matlab [M20] and it is shown there that this equation is indeed equal to zero, this means that x-coordinate is independent of the value of  $Z_{1T}$

The y-coordinate of the imaginary projector point source ( $y_{PST}$ ):

The same principle is used for the equation of  $y_{PST}$ , terms containing any form of  $Z_{1T}$  are made bold:

$$y_{PST} = 2 \frac{x_{pi1T} \tan(\omega) + y_{pi1T} - (\mathbf{Z}_{1T} + (90 - SD_p) - Z_{2T}) \tan^2(\omega)}{(\tan^2(\omega) + 1)} + 2 \frac{(\mathbf{Z}_{1T} + (90 - SD_p)) \tan^2(180^\circ - \psi)}{(\tan^2(180^\circ - \psi) + 1)}$$

The independency must result in the following equation:

$$2 \frac{x_{pi1T} \tan(\omega) + y_{pi1T} - (\mathbf{Z}_{1T} + (90 - SD_p)) \tan^2(\omega)}{(\tan^2(\omega) + 1)} + 2 \frac{(\mathbf{Z}_{1T} + (90 - SD_p)) \tan^2(180^\circ - \psi)}{(\tan^2(180^\circ - \psi) + 1)} = 0$$

This equation can be simplified when  $Z_{1T} + (90 - SD_p)$  is taken equal to A:

$$\begin{aligned} & 2 \frac{A \tan(180^\circ - \psi)}{(\tan^2(180^\circ - \psi) + 1)} \tan(\omega) - 2 \frac{A \tan^2(180^\circ - \psi)}{(\tan^2(180^\circ - \psi) + 1)} - A \tan^2(\omega) \\ & \frac{A \tan^2(180^\circ - \psi)}{(\tan^2(180^\circ - \psi) + 1)} = 0 \\ & \frac{2A \tan(180^\circ - \psi) \tan(\omega) - 2A \tan^2(180^\circ - \psi) - A \tan^2(\omega) (\tan^2(180^\circ - \psi) + 1)}{(\tan^2(\omega) + 1)A \tan^2(180^\circ - \psi)} \\ & + \frac{A \tan^2(180^\circ - \psi) (\tan^2(\omega) + 1)}{(\tan^2(\omega) + 1)(\tan^2(180^\circ - \psi) + 1)} = 0 \\ & 2A \tan(180^\circ - \psi) \tan(\omega) - 2A \tan^2(180^\circ - \psi) - A \tan^2(\omega) (\tan^2(180^\circ - \psi) + 1) \\ & + A \tan^2(180^\circ - \psi) (\tan^2(\omega) + 1) = 0 \end{aligned}$$

Dividing by A results in the following equation:

$$\begin{aligned} & 2 \tan(180^\circ - \psi) \tan(\omega) - 2 \tan^2(180^\circ - \psi) - \tan^2(\omega) (\tan^2(180^\circ - \psi) + 1) \\ & + \tan^2(180^\circ - \psi) (\tan^2(\omega) + 1) = 0 \\ & 2 \tan(180^\circ - \psi) \tan(\omega) - \tan^2(180^\circ - \psi) - \tan^2(\omega) = 0 \end{aligned}$$

This equation is also analyzed in the same Matlab [M20] and it is shown there that this equation is indeed equal to zero, this means that y-coordinate is also independent of the value of  $Z_{1T}$ .

### Conclusion

There can be concluded that  $Z_{2T}$  is the only parameter that affect the coordinates of the imaginary point sources and that these coordinates are independent of  $Z_{1T}$ .

#### IV. Appendix A4 Reducing the equations for the imaginary points sources

In Table A4.1 below the characteristics as introduced in Section 7.3.3 are summed up:

**Table A4.1** Overview of the parameters in the two systems

Parameters bottom system	Value	Parameters top system	Value
$\theta$	$45^\circ$	$\psi$	$90^\circ$
$\varphi$	$45^\circ$	$\omega$	$90^\circ$
$Z_{1B}$	$Z_{2B}$	$Z_{1T}$	eliminated ( <i>see Appendix III</i> )
$Z_{2B}$	$Z_B$	$Z_{2T}$	$Z_T$

Using the values of the parameters from table x reduces the obtained equations in Appendix II for the coordinates of the imaginary projector points sources. For the coordinates of the imaginary projector point source of the bottom mirror system ( $x_{PSB}$  and  $y_{PSB}$ ) this becomes:

$$x_{PSB} = 2 \frac{x_{pi1B} \tan^2(135^\circ) + (Z_B + (90 - SD_p) + y_{pi1B}) \tan(135^\circ)}{(\tan^2(135^\circ) + 1)} - 2 \frac{(Z_B + (90 - SD_p)) \tan(45^\circ)}{(\tan^2(45^\circ) + 1)}$$

$$x_{PSB} = 2 \frac{x_{pi1B} - (Z_B + (90 - SD_p) + y_{pi1B})}{2} - 2 \frac{(Z_B + (90 - SD_p))}{2}$$

$$x_{PSB} = x_{pi1B} - y_{pi1B} - 2Z_B - 2(90 - SD_p)$$

$$y_{PSB} = 2 \frac{x_{pi1B} \tan(135^\circ) + y_{pi1B} - (Z_B + (90 - SD_p)) \tan^2(135^\circ)}{(\tan^2(135^\circ) + 1)} + 2 \frac{(Z_B + (90 - SD_p)) \tan^2(45^\circ)}{(\tan^2(45^\circ) + 1)}$$

$$y_{PSB} = 2 \frac{-x_{pi1B} + y_{pi1B} - (Z_B + (90 - SD_p))}{2} + 2 \frac{(Z_B + (90 - SD_p))}{2}$$

$$y_{PSB} = -x_{pi1B} + y_{pi1B} - (Z_B + (90 - SD_p)) + (Z_B + (90 - SD_p))$$

$$y_{PSB} = -x_{pi1B} + y_{pi1B}$$

With:

$$x_{pi1B} = 2 \frac{(Z_B + (90 - SD_p)) \tan(45^\circ)}{(\tan^2(45^\circ) + 1)}$$

$$x_{pi1B} = (Z_B + (90 - SD_p))$$

$$y_{pi1B} = -2 \frac{(Z_B + (90 - SD_p)) \tan^2(45^\circ)}{(\tan^2(45^\circ) + 1)}$$

$$y_{pi1B} = -(Z_B + (90 - SD_p))$$

Combining this all gives:

$$x_{PSB} = 2 (Z_B + (90 - SD_p)) - 2Z_B - 2(90 - SD_p) = 0$$

$$y_{PSB} = -2 (Z_B + (90 - SD_p))$$

For the coordinates of the imaginary projector point source of the top mirror system ( $x_{PST}$  and  $y_{PST}$ ) this is a bit more difficult. This is caused by the fact that the equations contains terms with  $\tan(90^\circ)$ , the  $\tan(90^\circ) = \infty$  and therefore the equations will contain terms which will go to infinity. This means that these equations are therefore not directly usable. Limit theorems are needed in order to make these equations feasible. The elaboration of this is not mentioned in this report, but this would result in the following coordinates of the imaginary projector point source of the bottom system:

$$x_{PST} = 0$$

$$y_{PST} = 2Z_T$$

Summarizing, when the boundary conditions from Section 7.3.3 are fulfilled, the following equations for the coordinates of the imaginary projector point sources are obtained:

$$\begin{aligned} x_{PSB} &= 0 & x_{PST} &= 0 \\ y_{PSB} &= -2(Z_B + (90 - SD_p)) & y_{PST} &= 2Z_T \end{aligned}$$

These equations can be used in the coupling equation introduced in Section 7.3.3 to obtain a reduced coupling equation. Furthermore, these equations are used in Matlab [M11] and a visualization of the calculations is elaborated in a SolidWorks Model [S2]. This model will be explained using Figure A4.1.

Figure A4.1 shows the optical system according to the obtained coordinates in this appendix.

The figure shows two parameters, but only one parameter has to be chosen. The other one is obtained in the model by the reduced coupling equation (see Section 7.3). Therefore only the value of the top mirror system  $Z_{1T}$  is needed, in the figure this value is equal to 330 mm.

The coordinates of the imaginary point sources are encircled blue in the figure:

- Imaginary projector point source top: (0 ; 660)
- Imaginary camera point source top: (230,714 ; 697,096)
- Imaginary projector point source bottom: (0; -694,592)
- Imaginary camera point source bottom: (-230,714 ; -731,689)

The values in SolidWorks correspond with the values in Matlab [M11], this means that same input parameters result in equal coordinates for the imaginary point sources.

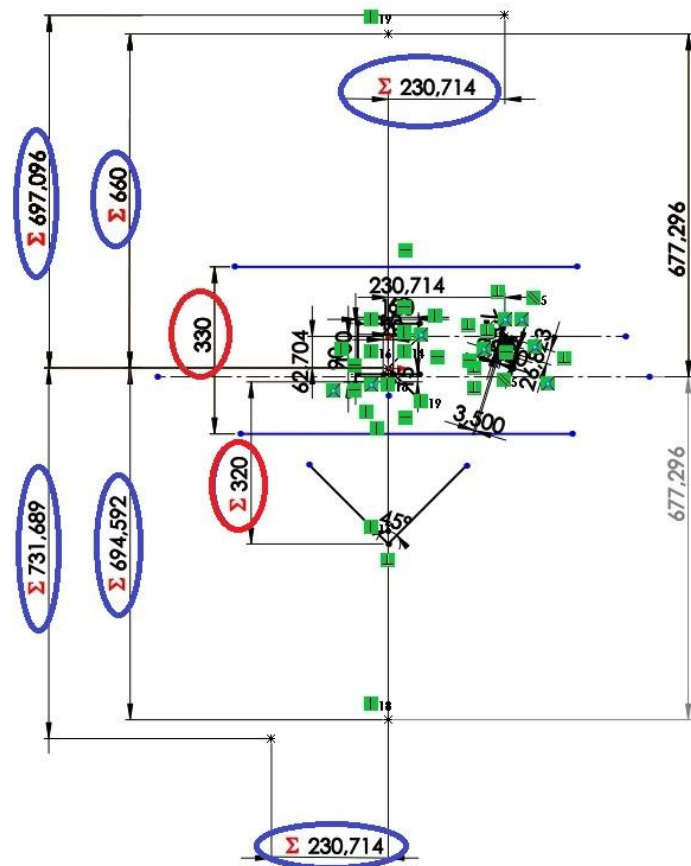


**Figure A4.1** Overview of the SolidWorks Model [S2], the input parameters are encircled red and the coordinates of the imaginary point sources are encircled blue (mm).

**V. Appendix A5 Calculation of the minimum and maximum first mirror distance**

It is important that the inner sides of the mirrors are installed exactly on the bisector of the beams. For the other side of the mirror there is not a direct restriction, the mirror must only reflect the total half of the beam and therefore there is not a maximum mirror size. However there is special case where the inner edges of the beams of the projector and the camera intersect at a certain  $h_1$  (the lines encircled with green in Figure A5.1).

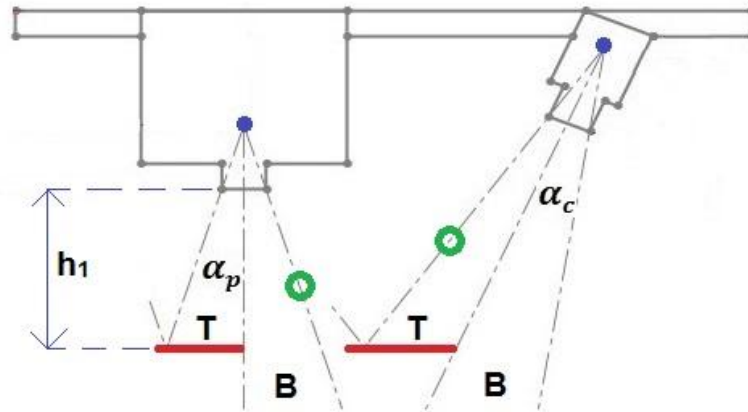


**Figure A5.1** Intended mirror setup at mirror position 1 such that the beams are splitted in half.

This has to be prevented because otherwise the beams for the bottom and top system cannot be separated, this gives a maximum value for  $h_1$ . This condition is elaborated in Matlab [M17], here mathematical equations for the lines are created to calculate in order to calculate the intersection point. This process resulted in the following maximum value of  $h_1$ :

$$h_{1max} = 238.1949 \text{ mm}$$

With these values it is also possible to calculate the dimensions of the mirrors at this maximum mirror distance  $h_{1max}$ . This is done using Figure A5.2 and A5.3, these figures represent the views needed for the calculations of respectively the width and the height of the mirrors. The listed values in the figures are measured dimensions of the projector and the scanning setup.

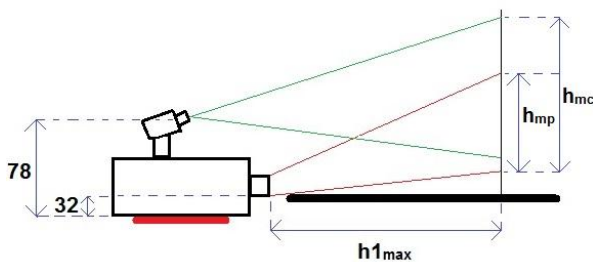


**Figure A5.2** Side view with the mirror heights

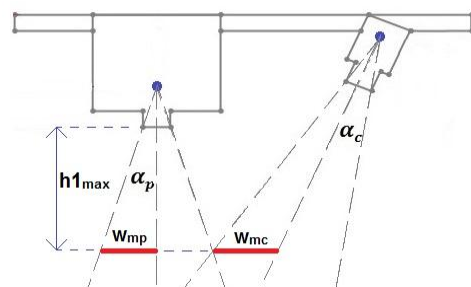


**Figure A5.3** top view with the mirror widths

The calculations of these two mirrors dimensions are done in Matlab [M17]. For the mirror heights the heights are calculated with the boundary equation that the mirrors will be inclined at the same horizontal plane, see Figure A5.2. Furthermore, the camera and the projector are installed according to the properties needed for the situation of a scanning distance at 650 mm (E). This property leads to a vertical inclining angle for the camera (this is needed for the capturing of the tilted projection area as discussed in Section 4.1), this is also visible in the figure. The calibration process gives the inclining angles of the camera, this is shown in Figure A5.4.

This figure gives for the vertical angle ( $\xi$ )  $4.61^\circ$  (and for the inclining angle ( $\lambda$ )  $90^\circ - 17.09^\circ = 72.27^\circ$ , which approaches the mathematical value in Section 5.5 pretty well). This calculations in the Matlab script [M17] resulted in the following maximum dimensions:

Height ( $h_{mp}$ ) and width ( $w_{mp}$ ) of the mirror needed for the projector reflection:  
 $h_{mp} = 89.0576 \text{ mm}$        $w_{mp} = 57.8714 \text{ mm}$

Height ( $h_{mc}$ ) and width ( $w_{mc}$ ) of the mirror needed for the camera reflection:  
 $h_{mc} = 117.1652 \text{ mm}$        $w_{mc} = 70.5195$

**Note:**

The dimensions of the scanning system that will be used during the following calculations are shown in Figure A5.5. The values are measured and are illustrated in mm. These values are also the input parameters for Matlab [M17,M18]

However, the reflections by the first mirrors have to be reflected back to the second mirror which is located behind the scanning system. But, this means that the projection beam need to trespass over the projector as illustrated in Figure A5.6. The calculations are done in Matlab [M17] and gave the following results for this case:

$$h_{1min} = 295.4376 \text{ mm}$$

Comparing the values of  $h_{1min}$  and  $h_{1max}$  results in the conclusion that this is physically impossible because  $h_{1min}$  is larger than  $h_{1max}$ . Furthermore, the value of  $h_{1max}$  is too large because this would result in a scanning distance which is larger then the set 650 mm (E).

So this means that a new value physically possible value for  $h_{1max}$  has to be determined. This value can be determined using the condition that the second mirror is as close as possible behind the projector and the projection area collapse with the first mirror (green dotted line in Figure A5.7).

$$h_{1max} = \frac{E - (2 \times 115)}{3} = 140 \text{ mm}$$

This results in the following maximum and minimum value of the mirror distance:

$$h_{1max} = 140.0000 \text{ mm}$$

$$h_{1min} = 295.4376 \text{ mm}$$

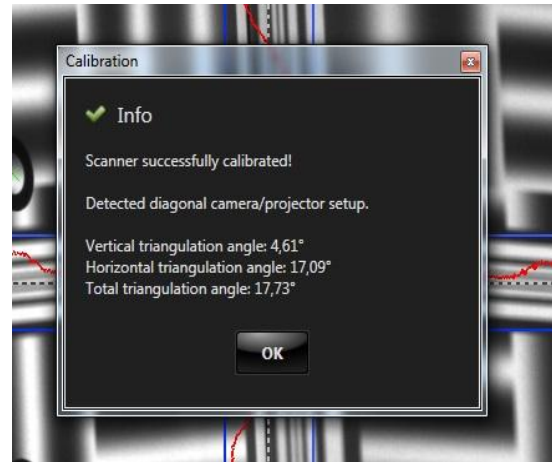


Figure A5.4 Calibration window DAVID

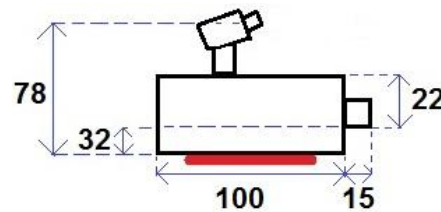


Figure A5.5 Calibration window DAVID

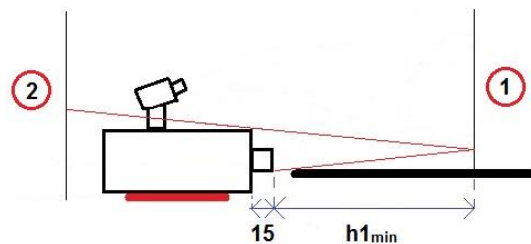


Figure A5.6 Side view with the minimum distance

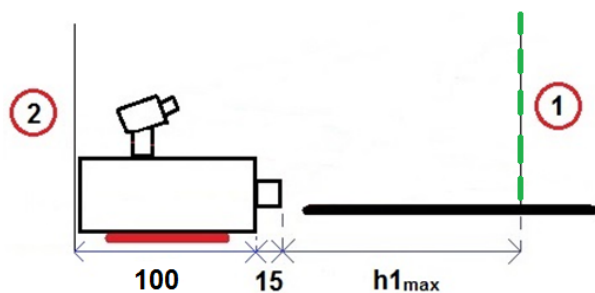
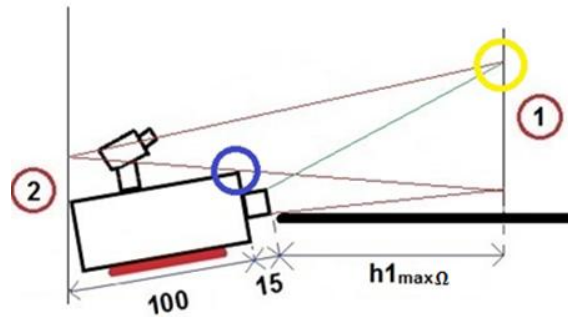


Figure A5.7 Side view with the maximum distance

**VI. Appendix A6 Calculation of the minimum vertical tilt angle**

In order to realize the total system the whole scanning system needs to be tilted under a vertical angle. This vertical angle is an extra degree of freedom and it has to achieve that the value of  $h_{1min}$  becomes smaller than  $h_{1max}$ . This condition is translated into two boundary conditions as illustrated in Figure A6.1. During the analyzes there is assumed that the bottom side of the projector lens is against the edge of a horizontal surface, such as a table, and that  $h_1$  is measured from this point. This enables the positioning of the different components by distances measured on the table surface.



**Figure A6.1** Top mirror system with the minimum vertical tilt angle and two boundary situations

In the figure the following two boundary situations can be seen:

- The intersection of the highest ray of the projection with the second mirror reflection of the lowest projection ray. In this case the mirror at position one is high enough to reflect the whole range of the projection but does not block the intended reflections, encircled with yellow in the figure.
- The situation where the lowest projection ray intersect with the top side of the projector, encircled with blue in the figure.

To calculate the minimum tilt angle needed to fulfill both situations, the distance  $h_1$  needs to be specified. The minimum required angle reduces for increasing distance  $h_1$ . A larger tilt angle means that the image of the hand will contain less detail as concluded in Section 6.2.2. Therefore there is assumed that a maximum tilt angle of  $20^\circ$  is still permissible. This assumption leads to a maximum mirror distance  $h_{1max\Omega}$ . This value arises out of the two obtained values of  $h_{1max}$  calculated in Appendix V.

The vertical angle of  $20^\circ$  affects the horizontal scanning distance. Before this horizontal distance was equal to the scanning distance  $E$ . However the tilting of the scanning system reduces this distance, this is illustrated in Figure A6.2.

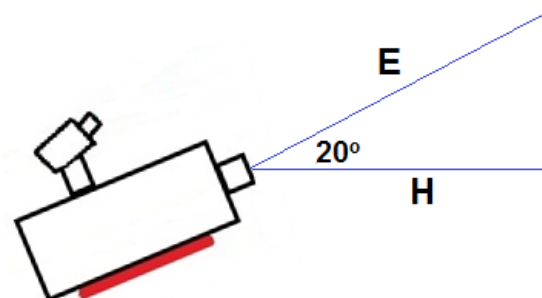


**Figure A6.2** Adaptation of the scanning distance

The horizontal scanning distance  $H$  in case of a vertical angle of  $20^\circ$  can now be calculated:

$$H = \cos(20^\circ) \times E = 610.800 \text{ mm}$$

This principle affects the two boundary conditions in Appendix V that determined the value of  $h_{1max}$ . The calculations for the maximum mirror distance  $h_{1max\Omega}$  in case of the vertical angle of  $20^\circ$  are done in Matlab [M18]. This resulted in the following distance:

$$h_{1max\Omega} = 125.8623 \text{ mm}$$

Using this maximum distance to the first mirror makes it is possible to calculate the minimum tilt angles for the two discussed situations in Figure A6.1. The minimum angle for the first situation can be obtained by determining the characteristics of the lowest projection ray (which is reflected by the

first and the second mirror) to the first mirror and the characteristics of the highest projection ray which is sent directly to the first mirror (see Figure A6.1). When the heights of the intersection points of these rays on the first mirror are known, it is possible to calculate when these heights are equal. This gives the minimum required vertical angle. The second situation can be elaborated using the same principles as is done in Appendix V, but know the mirror distance is set and the vertical angle is the unknown property. These two situations are elaborated in Matlab [M18]. In these calculations there is made use of the fact that  $\cos \alpha = 1/\sqrt{\tan^2 \alpha + 1}$  and  $\sin \alpha = \tan \alpha / \sqrt{\tan^2 \alpha + 1}$ . This resulted in the following two minimum vertical angles:

$$\Omega_1 = 3.8515^\circ \text{ and } \Omega_2 = 2.4770^\circ$$

Therefore the minimum tilt angle  $\Omega$  becomes  $3.8515^\circ$  to ensure that both of the conditions are fulfilled. Also a Solidworks model is created to give more insight in the effects of the vertical rotation of the scanning system [S3]. This model confirms the correctness of the calculated values for the mirror distance and the minimum tilt angles. An overview of this model is shown in Figure A6.3.

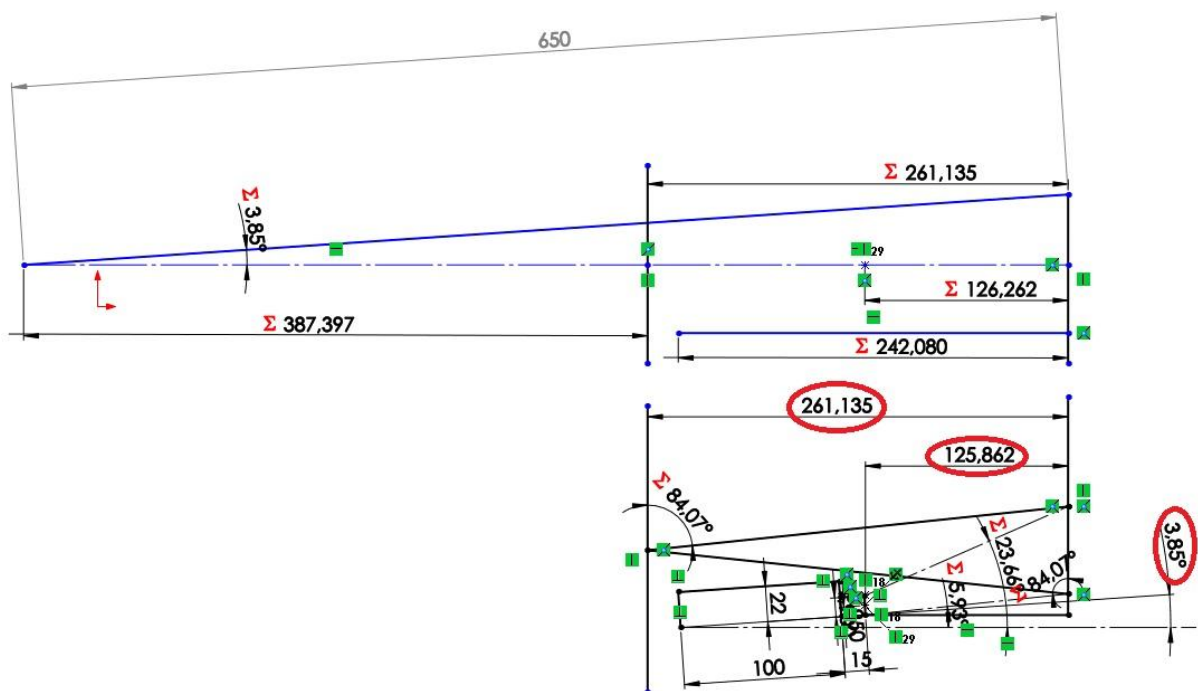


Figure A6.3 Overview of the vertical angle model in Solidworks [S3]

In this figure three values are encircled, these are the values that are adjustable and determine the characteristics of the scanning system. These are the vertical angle  $\Omega$ , the distance to the first mirror  $h_1$  and the distance between the two top mirrors  $Z_B$  (the figure shows the correctness of the second boundary situation).

Using the obtained minimum vertical tilt angle  $\Omega$  and the intersection points of the projector and camera rays on the first mirrors makes it possible to calculate the maximum mirror dimensions; this is illustrated in Figure A6.4. The same principle is used as in Appendix V, only the scanning system is now tilted under the vertical angle  $\Omega$ . These calculations are again performed in Matlab [M18].

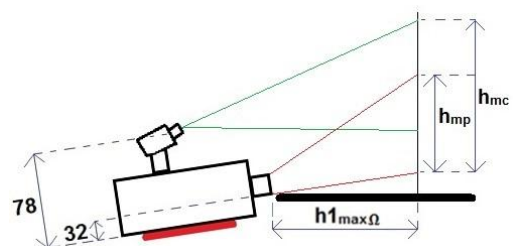


Figure A6.4 Reflection points on the first mirror with the heights of the two mirrors  $h_{mp}$  and  $h_{mc}$ .